NEOPLASIA
www.neoplasia.com
Volume 14 Number 12 December 2012 pp. 1236–1248 1236

Regeneration-associated WNT Signaling Is Activated in Long-term Reconstituting AC133^{bright} Acute Myeloid Leukemia Cells[1,2]

Alessandro Beghini*, Francesca Corlazzoli*,[3], Luca Del Giacco†,[3], Matteo Re‡, Francesca Lazzaroni*, Matteo Brioschi§, Giorgio Valentini‡, Fulvia Ferrazzi¶,#, Anna Ghilardi†, Marco Righi*,, Mauro Turrini††, Marco Mignardi‡‡,§§, Clara Cesana††, Vincenzo Bronte¶¶, Mats Nilsson‡‡,§§, Enrica Morra†† and Roberto Cairoli††,##**

*Department of Medical Biotechnology and Translational Medicine, Università degli Studi di Milano, Milano, Italy; †Department of Biosciences, Università degli Studi di Milano, Milano, Italy; ‡Department of Computer Science, Università degli Studi di Milano, Milano, Italy; §Dipartimento di Scienze Oncologiche e Chirurgiche, Università degli Studi di Padova, Padova, Italy; ¶Dipartimento di Informatica e Sistemistica, Università degli Studi di Pavia, Pavia, Italy; #Gene Center, Ludwig-Maximilians-Universität München, Munich, Germany; **Consiglio Nazionale delle Ricerche, Institute of Neuroscience, Milano, Italy; ††Department of Oncology, Niguarda Hospital, Milano, Italy; ‡‡Department of Immunology, Genetics and Pathology, Rudbeck Laboratory, Uppsala Universitet, Uppsala, Sweden; §§Science for Life Laboratory, Department of Biochemistry and Biophysics, Stockholm University, Solna, Sweden; ¶¶Istituto Oncologico Veneto, Padova, Italy; ##Divisione di Medicina Interna, Sezione di Ematologia Clinica, Ospedale Valduce, Como, Italy

Abstract

Acute myeloid leukemia (AML) is a genetically heterogeneous clonal disorder characterized by two molecularly distinct self-renewing leukemic stem cell (LSC) populations most closely related to normal progenitors and organized as a hierarchy. A requirement for WNT/β-catenin signaling in the pathogenesis of AML has recently been suggested by a mouse model. However, its relationship to a specific molecular function promoting retention of self-renewing leukemia-initiating cells (LICs) in human remains elusive. To identify transcriptional programs involved in the maintenance of a self-renewing state in LICs, we performed the expression profiling in normal (n = 10) and leukemic (n = 33) human long-term reconstituting AC133^{+} cells, which represent an expanded cell population in most AML patients. This study reveals the ligand-dependent WNT pathway activation in AC133^{bright} AML cells and shows a diffuse

Abbreviations: AML, acute myeloid leukemia; LSC, leukemic stem cell; LT-HSCs, long-term hematopoietic stem cells; CFU, colony forming units; CFU-GM, granulocyte/macrophage; BM MNCs, bone marrow mononuclear cells; LIC, leukemia-initiating cell

Address all correspondence to: Alessandro Beghini, PhD, Department of Medical Biotechnology and Translational Medicine, Università degli Studi di Milano, via Viotti 3/5, 20133 Milano, Italy. E-mail: alessandro.beghini@unimi.it

[1]This work was supported in part by PUR 2008 (to A.B.), Progetto Integrato Oncologia 2006 (RO 4/2007), Associazione Malattie del Sangue Onlus (AMS), and Piano Regionale Sangue-Regione Lombardia 2006 (DDG 7917). The authors declare that they have no competing financial interests.
[2]This article refers to supplementary materials, which are designated by Table W1 and W2 and Figure W1 and are available online at www.neoplasia.com.
[3]F. Corlazzoli and L. Del Giacco contributed equally to this work.
Received 7 September 2012; Revised 15 October 2012; Accepted 18 October 2012

DOI 10.1593/neo.121480

expression and release of WNT10B, a hematopoietic stem cell regenerative-associated molecule. The establishment of a primary AC133$^+$ AML cell culture (A46) demonstrated that leukemia cells synthesize and secrete WNT ligands, increasing the levels of dephosphorylated β-catenin *in vivo*. We tested the LSC functional activity in AC133$^+$ cells and found significant levels of engraftment upon transplantation of A46 cells into irradiated Rag2$^{-/-}\gamma c^{-/-}$ mice. Owing to the link between hematopoietic regeneration and developmental signaling, we transplanted A46 cells into developing zebrafish. This system revealed the formation of ectopic structures by activating dorsal organizer markers that act downstream of the WNT pathway. In conclusion, our findings suggest that AC133^{bright} LSCs are promoted by misappropriating homeostatic WNT programs that control hematopoietic regeneration.

Neoplasia (2012) 14, 1236–1248

Introduction

Different genetic causes result in variable clinical courses of acute myeloid leukemia (AML) and different responses to standard chemotherapy including stem cell transplant. Despite the genetic differences among individual patients, most AML clones display certain common features. Ample evidence exists in mouse models that AML develops through the stepwise acquisition of collaborating genetic and epigenetic changes in self-renewing LICs, which exhibit a committed myeloid immunophenotype and give rise to nonleukemogenic progeny in a myeloid-restricted hierarchy [1–3]. An important issue to understand the early events in the origin of AML is the observation that long-term hematopoietic stem cell (LT-HSC) expansion precedes the generation of committed myeloid LICs [4].

Although well-orchestrated cell intrinsic programs and environmental cues represent the main contributory factors for normal LT-HSC expansion, it is still unclear if transcriptional programs responsible for the expansion of premalignant LT-HSC populations and leukemia initiation share common embryonic or post-embryonic functions, such as stem cell renewal, tissue repair, and regeneration [5,6]. Even though recent studies have addressed the role of Hedgehog signaling for maintenance of cancer stem cells in myeloid leukemia [7], its requirement in AML remains controversial [8].

Recently, the notion that LICs are restricted only to the CD34$^+$CD38$^-$ population has been challenged [9,10] and it has been suggested that more cell surface markers could be appropriately used to enrich the leukemia-initiating cell (LIC)–containing fraction. One of such markers is the AC133 antigen (a glycosylation-dependent epitope of CD133) that defines a desirable population of stem and progenitor cells containing in turn all the CD34^{bright}CD38$^-$ progenitors, as well as the CD34^{bright}CD38$^+$ cells committed to the granulocytic/monocytic lineage [11]. In addition, AC133 represents a well-documented marker of tumor-initiating cells in a number of human cancers [12]. In this study, fluorescence-activated cell sorter (FACS) analysis demonstrates that AC133$^+$ cell population is dramatically expanded in 25 AML cases analyzed. We carried out genome-wide transcriptional analysis of AC133$^+$ cells isolated from newly diagnosed non-promyelocytic AML patients (n = 33) and healthy donors (n = 10). Results obtained from a multistep analysis of the generated data defined the involvement of the ligand-dependent WNT receptor signaling pathway as the self-renewal associated signature in the AC133-enriched fraction in human AML. Furthermore, the results presented here suggested that *WNT10B* and other WNT genes expressed during the regenerative process of the hematopoietic system [13,14] are aberrantly upregulated in AC133^{bright} AML cells. To obtain a localized detection of each single transcript, we first applied an *in situ* detection of individual mRNA molecules [15] on bone marrow (BM) sections from AML patients. By the establishment of a primary culture of AC133$^+$ AML cells (termed A46 hereafter), we confirmed that secreted WNTs activated a β-catenin/human T-cell factor (TCF) transcription–based reporter construct. Moreover, we intend to clarify the relationship between the abnormal WNT activation in AC133$^+$ population and the leukemic stem cell (LSC) activity. Using Rag2$^{-/-}\gamma c^{-/-}$ as immunodeficient xenotransplant model [16], AC133$^+$ A46 cells were injected intravenously into sublethally irradiated mice.

To achieve a complete view of how AC133$^+$ A46 cells modulated the microenvironment and given that hematopoietic regeneration converge to developmental signaling, we used zebrafish embryonic model as an *in vivo* biosensor.

Our results confirmed previously reported data [17] and raise new important implications for the involvement of the ligand-dependent canonical WNT pathway in AML. These suggestive findings are supported by the pivotal function of WNT in promoting self-renewal [18,19], its emerging role in myeloid leukemogenesis [20,21], and the effects of its constitutive activation through a stabilized form of β-catenin, by inducing quiescent stem cells to enter the cell cycle and arresting their differentiation [22,23].

Materials and Methods

Collection of Patient Samples and Normal Hematopoietic Cells

BM MNCs were collected from 33 newly diagnosed, unselected non-promyelocytic AML patients, according to Niguarda Hospital's Ethical Board–approved protocols (116_04/2010). According to the revised Medical Research Council risk group stratification, based on cytogenetic and molecular markers/mutations [24], samples included 14 adverse, 13 intermediate, and 6 favorable risk patients. Human adult BM cells obtained from 10 consenting healthy donors were processed as previously described [25].

Cell Sorting and Flow Cytometry

We carried out AC133$^+$ cell separation based on MACS MicroBeads and cytofluorometric determinations, as previously described [25].

Microarray Expression Analysis

Total RNA for expression profiling was extracted using RNAqueous-4PCR kit (Ambion, Austin, TX) from AC133-selected cells. Expression profiling was performed on Affymetrix HGU133plus2.0 GeneChip

arrays according to the manufacturer's procedures. The bioinformatics analysis performed in this study was realized using the R language for statistical computing (http://www.r-project.org/) and the annotation libraries provided by the Bioconductor project (http://www.bioconductor.org/). Microarray data have been deposited in ArrayExpress (http://www.ebi.ac.uk/arrayexpress/), with accession number E-MTAB-220. We performed a genome-wide analysis to select genes differentially expressed between AML AC133+ patients and AC133+ healthy donors (Welch *t* test, 0.05 significance level). The resulting set of differentially expressed genes has been analyzed for functional enrichment with respect to the terms of the Biological Process (BP) branch of the Gene Ontology (GO) and the pathways of the KEGG database. We relied on three different methods for functional enrichment analysis: GOStats (version 2.12.0 of the Bioconductor package, http://www.bioconductor.org/packages/release/bioc/html/GOstats.html) [26], Database for Annotation, Visualization and Integrated Discovery (DAVID; http://david.abcc.ncifcrf.gov/home.jsp) [27], and the iterative procedure of dysregulated pathway analysis proposed by Majeti et al. [17]. The first two tests are based on the hypergeometric distribution, whereas the last one is based on a non-parametric test and on an iterative procedure. Overrepresented GO terms and KEGG pathways have been selected at 0.05 significance level.

WNT/β-catenin Responsive Luciferase Assay

HEK293T cells grown in 24-well plates at a density of 1.7×10^5 cells per well were transfected with M50 Super 8x TOPFlash (plasmid 12456; Addgene, Cambridge, MA) and pRL-TK (Renilla luciferase; Promega, Madison, WI) using jetPEI (Polyplus, New York, NY). Cells were treated for 12 hours with A46 conditioned medium (CM) or HEK293T cells transfected with BA-*WNT10B* (plasmid 1831; Addgene) CM as positive control. *WNT10B* expression in HEK293T transfected with BA-WNT10B was evaluated by SYBR Green–based real-time reverse transcription–polymerase chain reaction (RT-PCR) using *WNT10B* FW-5′-GCTGTAACCATGACATGGAC-3′ and RW-5′-CTGCCTGATGTGCCATGAC-3′ specific primers. Luciferase activity measurement was performed with the Dual-Luciferase Reporter Assay System (Promega).

Immunoblot

Protein expression was assessed by immunoblot analysis using standard procedures, applying anti–active β-catenin (ABC) monoclonal mouse (anti-ABC clone 8E7; Millipore, Billerica, MA), anti–β-catenin monoclonal rabbit (E247; Abcam, Cambridge, United Kingdom), anti–WNT10B polyclonal rabbit (H-70; Santa Cruz Biotechnology, Inc, Santa Cruz, CA), anti–WNT10B monoclonal mouse (5A7; Abcam), anti–glyceraldehyde-3-phosphate dehydrogenase (GAPDH) polyclonal rabbit (ab97626; Abcam), and anti–Pygopus 2 polyclonal rabbit (H-216; Santa Cruz Biotechnology, Inc) antibodies. Secondary antibodies used were anti–mouse HRP, anti–goat HRP, and anti–rabbit HRP (Thermo Fisher Scientific, Waltham, MA).

In Situ *mRNA Detection*

In situ detection of individual mRNA molecules was performed as described [15]. One micromolar of locked nucleic acid–modified cDNA primer (*WNT10B*, 5′-C+A+G+G+C+CGGACAGCGTCAAGCACACG-3′; *β-actin*, 5′-C+TG+AC+CC+AT+GCCCACCATCACGCCC-3′; Exiqon, Vedbaek, Denmark) was added to the reverse transcriptase reaction. Ligation was then carried out with 0.1 μM of the *WNT10B* padlock probe or *β-actin* padlock probe (*WNT10B*, 5′-[Phos]ACCGTGCCTGTCGGACCCTCCTCTATGATTACTGACCTAAGTCGGAAGTACTACTCTCTTCTTCTTTTAGTGAAGCCCAGGCAACCCA-3′; *β-actin*, 5′-[Phos]GCCGGCTTCGCGGGCGACGATTCCTCTATGATTACTGACCTATGCGTCTATTTAGTGGAGCCTCTTCTTTACGGCGCCGGCATGTGCAAG-3′; Sigma-Aldrich, St Louis, MO). Rolling circle products (RCPs) were visualized using 100 nM of detection probe (*WNT10B*, 5′-Cy5-AGTCGGAAGTACTACTCTCT-3′ and *β-actin*, 5′-Cy3-TGCGTCTATTTAGTGGAGCC-3′; Sigma-Aldrich). Nuclei were counterstained with 100 ng/ml Hoechst 33258 (Sigma-Aldrich). Images of BM tissue slides were acquired using an Axioplan II epifluorescence microscope (Zeiss, Munchen, Germany) equipped with a charge-coupled device (CCD) camera (HRM, Zeiss) and a computer-controlled filter wheel with excitation and emission filters for visualization of 4′-6-diamidino-2-phenylindole (DAPI), Cy3, and Cy5. A ×20 objective (Plan-Apocromat, Zeiss) was used for capturing the images. Images were collected using the Axiovision software (release 4.3, Zeiss). Images were collected as *z*-stacks to ensure that all RCPs were imaged, with a maximum intensity project created in Axiovision. For quantification, the numbers of RCPs and cell nuclei in images were counted digitally using CellProfiler software (www.cellprofiler.org) on three ×20 microscope images. The total number of RCPs was divided by the number of nuclei for each image. The average for each sample was then calculated from the result of the three images and is reported as RCPs per cell.

Immunostaining

Direct and indirect immunostaining were performed following standard procedures. BM biopsies of AML patients, previously embedded in paraffin blocks, were cut in 5-μm-thick sections and mounted on slides. Slides were incubated with primary antibody mouse anti-CD133.1 (AC133) (1:100; Miltenyi Biotec GmBH, Bergisch Gladbach, Germany), directly labeled with 488-nm dye (Sigma), and with primary antibodies such as mouse anti-ABC (1:100; Millipore), rabbit anti-WNT10B (H70) (1:100; Santa Cruz Biotechnology, Inc), rabbit anti–Pygopus 2 (H-216) (1:100; Santa Cruz Biotechnology, Inc), goat anti-SMYD3 (F-19) (1:100; Santa Cruz Biotechnology, Inc). Samples were incubated with the secondary antibodies donkey anti-mouse Alexa Fluor 488 (1:500; Life Technologies, Carlsband, CA), donkey anti-rabbit Alexa Fluor 568 (1:500; Life Technologies), and donkey anti-goat Alexa Fluor 568 (1:500; Life technologies). Nuclei were counterstained with 100 ng/ml DAPI (Sigma-Aldrich). Cells were analyzed using the upright microscope (Leica, DM 4000B).

Immunofluorescence Image Analysis

Image analysis was performed by means of a custom automatic routine and the ImageJ program (1.43s; National Institutes of Health, Bethesda, MD). Maps of ABC+/WNT10B+ cells were obtained using an automatic threshold based on moments algorithm newly implemented in the ImageJ program and mathematical morphology plugin developed by D. Prodanov (http://rsbweb.nih.gov/ij/plugins/gray-morphology.html). DAPI staining was used to identify nuclei. Finally, images of nuclei for positive cells were obtained by Boolean AND operations between DAPI staining and cell maps. The resulting images were used to determine the percentage of ABC+/WNT10B+ cells both manually or through the Analyze Particles function of ImageJ.

Cell Culture

Selected AC133+ cells from BM at AML diagnosis were cultured for 16 weeks. The culture was performed using synthetic medium

StemSpam H3000 (StemCell Technologies, Vancouver, Canada) in the absence of serum and cytokines. StemSpan H3000 and HPGM media, conditioned by the cell culture, were collected after 12 weeks, refined with 0.2-μm filter and stored at −20°C. HEK293T cells were grown in Dulbecco's modified Eagle's medium (high glucose with sodium pyruvate and L-glutamine; Euroclone), supplemented with 10% FBS (Euroclone) and penicillin-streptomycin solution (100×) (Euroclone, Milano, Italy).

Mice and Xenogeneic Transplantation

Rag2$^{-/-}\gamma c^{-/-}$ BALB/c mice were bred and maintained under specific pathogen-free conditions in the mouse facility of Istituto Oncologico Veneto, and experiments were performed according to state guidelines and approved by the local ethics committee. Rag2$^{-/-}\gamma c^{-/-}$ mice at 6 weeks were sublethally irradiated with 5 Gy and transplanted via the tail vein with 1×10^6 of human AC133$^+$ AML cells (A46).

Evaluation of Hematopoietic Chimerism by Flow Cytometry

Three weeks after transplantation, recipient mice were sacrificed and BM cells were harvested by flushing femurs and tibias. BM engraftment was evaluated using human antibodies CD34, CD38, AC133, and CD45 [BD Biosciences (Bedford, MA) and Miltenyi Biotec GmBH]. Multicolor flow cytometric analyses were performed using FACSCalibur flow cytometer (BD Biosciences) and analyzed by FlowJo software (Tree Star, Ashland, OR). Cell engraftment was determined by expression of the human panleukocyte marker CD45.

Zebrafish Models and Transplantation Procedures

Embryos were handled according to relevant guidelines. Fish of the AB strain were maintained at 28°C on a 14-hour light/10-hour dark cycle and collected by natural spawning. Transplantation of human A46 cells into zebrafish embryos was performed as previously reported [28]. Briefly, fluorescently labeled A46 cells were resuspended in 1× phosphate-buffered saline and injected into zebrafish blastulae (between 100 and 200 cells per injection) at 3 hours post-fertilization (hpf). Injected live embryos were observed under a fluorescent microscope at 30% of epiboly to ensure the presence of labeled A46 cells. Embryos were collected at the desired developmental stages, immediately fixed, and processed for whole-mount *in situ* hybridization according to Thisse et al. [29], using *gsc*, *ntl*, and *pax2a* DIG-labeled riboprobes.

Results

AC133$^+$ Cells Are Highly Expanded in AML

AC133 antigen is restricted to a rare cell population with long-term reconstituting activity, ranging from 20% to 60% of all CD34$^+$ cells, and resulting barely detectable in CD34$^-$Lin$^-$ cells [11–30]. We have previously shown that AC133$^+$ LT-HSCs are also highly enriched in colony forming units and have a stronger granulocyte/macrophage differentiation potential relative to unselected BM MNCs. However, their burst-forming units–erythroid forming potential is lower [25]. To determine the range of expansion of AC133$^+$ cell fraction in AML, flow cytometric quantification of CD133.1 (AC133) expression either in single staining or in combination with the pan-hematopoietic marker CD45 was performed in BM on 25 primary non-promyelocytic AML samples and 10 age-matched healthy volunteer adult donors. The resulting CD133.1$^+$ cell fraction results expanded among AML patients by a median of 31.5% [interquartile range (IQR), 16.5%–53.4%] with respect to normal donors (median, 0.54%; IQR, 0.17%–1.14%; $P <$ .0001; Figure 1, *A–C*). To directly compare the gene expression profiles of purified populations highly enriched in LSCs or HSCs, positive selection of CD133.1$^+$ cells was performed on all the 33 non-promyelocytic AML patients (25 *de novo*, 7 secondary to myelodysplasia, and 1 secondary therapy-related; Table W1) as well as on the 10 healthy donors recruited to this study, respectively. MNC selection in samples from AML patients led to an average of 236-fold enrichment of AC133-positive cells (IQR, 142.72–419.44, data not shown).

Identification of Dysregulated Pathways in AC133$^+$ AML Cell Fraction

To identify the dysregulated pathways in AC133$^+$ AML cell fraction *versus* normal long-term reconstituting AC133$^+$ HSC cells, we performed a genome-wide functional enrichment analysis on gene expression microarray data of 33 AML patients and 10 healthy donors. The identification of overrepresented pathways in AC133$^+$ AML cells was realized through three computational tools: GOStats [26], DAVID [27], and dysregulated pathway analysis according to Majeti et al. [17]. Employing the functional terms from GO BPs and the pathway information from KEGG databases, we found 212 functionally enriched GO BP terms with GOStats ($P < .01$), 284 GO BP terms with DAVID ($P < .05$), and 616 GO BP terms with the non-parametric test of Majeti et al. ($P < .05$). Moreover, GOStats selected 16 KEGG pathways

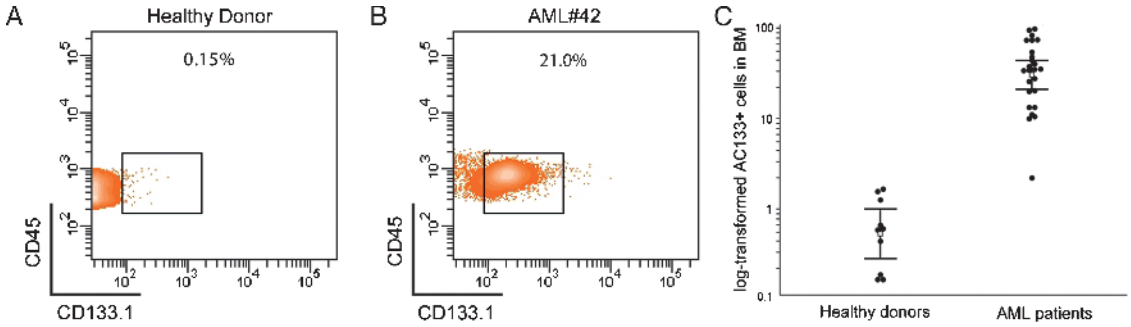

Figure 1. Human AC133$^+$ cells are strongly expanded in AML. Representative dot plots of the immunophenotype analysis from the BM of (A) a healthy donor and (B) a patient with AML (AML No. 42 in Table W1). The CD45/CD133.1 co-staining was gated on BM MNCs; percentages on total cellularity are shown for gated normal and AML populations. (C) Flow cytometry analysis of the CD133.1 antigen in BM MNCs of healthy donors ($n = 10$) and AML patients ($n = 25$). The IQR for each sample group is indicated in the dot. Mann-Whitney *U* test was used to calculate the *P* value ($\alpha = 0.001$).

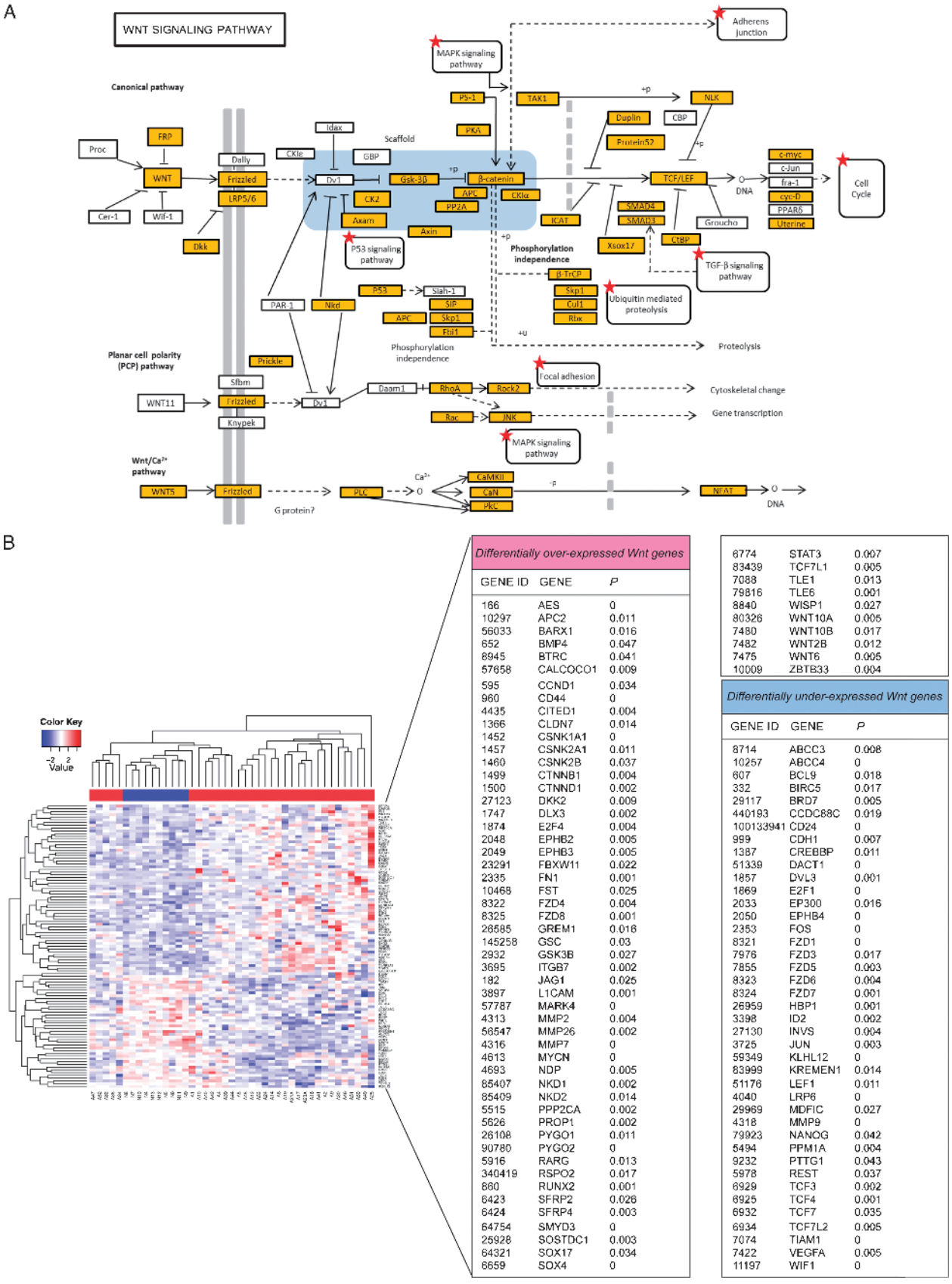

Figure 2. Schematic visualization of dysregulated networks in KEGG database and representation of WNT gene expression profiles. (A) Visualization of WNT signaling pathway in the KEGG database. Highlighted genes are differentially expressed and red-starred pathways are overrepresented in AC133+ AML cells. (B) Heat map of the differentially expressed WNT-associated genes. The color bar under the patient sample dendrogram identifies AML samples (red) and healthy controls (blue). The names, accession numbers, as well as *P* values for the differentially overexpressed and underexpressed genes are shown in the right panels.

($P < .05$), DAVID selected 24 KEGG pathways ($P < .05$), and the dysregulated pathway analysis selected 3 KEGG pathways ($P < .05$). As shown in Table W2, DAVID ranks the WNT signaling pathway ($P = .022$) among the first 10 dysregulated pathways in AC133$^+$ AML cells. The visualization of the WNT molecular interaction in KEGG database is presented in Figure 2*A*.

It is worth noting that different statistical methods agree in identifying the WNT pathway as a significant dysregulated pathway in AC133$^+$ AML cells. Moreover, the WNT signaling pathway in KEGG is selected as overrepresented in AC133$^+$ AML stem cells by both GOStats and DAVID. Taken together, the functional enrichment methods select the term "WNT receptor signaling pathway" (GO:0016055) as the most specific self-renewal associated dysregulated pathway.

WNT Gene Expression Profiles of Normal and Leukemia Long-term Reconstituting AC133$^+$ Cells

To obtain insights into the WNT pathway in AC133$^+$ leukemia cells, we focused our analysis on the probe sets annotated to "WNT receptor signaling pathway" GO class or to any of its children GO terms. The resulting probe set list was complemented with the probes mapping to genes in a manually curated list of WNT target genes and with probes mapping to other well-known WNT genes, not included in the previous two lists. The total list of analyzed WNT genes includes 480 probe sets, mapping to 193 different genes (Table_A in http://homes.dsi.unimi.it/~re/TRdataset/). To assess differential expression of WNT genes, we employed Welch *t* tests (two-tailed) on the 480 probe sets, thus identifying 103 differentially expressed genes ($P < .05$; Figure 2*B*). Genes shown to be highly AML-specific include the WNT ligands *WNT2B*, *WNT6*, *WNT10A*, and *WNT10B* [14], the WNT/β-catenin signaling agonists including *SMYD3* [31], *DKK2* [32], *SOX4* [33], *PROP-1* [34], and *PYGO2* [35,36], antagonists including *WIF-1* [37], *KLHL12* [38], *LRP6* [39], *KREMEN1* [40], *E2F1* [41], *DACT1* [42], and *HBP1* [43], and the deregulated WNT targets including *STAT3*, *MYCN*, *ABCC4*, *DLX3*, *MARK4*, *RUNX2*, *CD24*, and *CD44* [44]. Collectively, these data are consistent with ligand-dependent activation of the regeneration-associated WNT pathway [14].

We also investigated whether the expression of the WNT genes varied between the risk groups in AML (favorable, intermediate, and adverse) revised by Smith et al. [24]. Clustering results of AML cases restricted to WNT genes show that the risk groups are not clearly distinguishable in separate clusters (Figure 2*B*). Analysis of variance between groups confirms these results: only 3 (*ABCC4*, *HBP1*, and *NDP*) of 193 WNT-related genes are differentially expressed across the three categories ($P < .05$). Thus, our data do not support a significant distinction between risk groups in AML patients. This statement should be considered with caution, because the cardinality of the subgroups is relatively low (6 favorable, 13 intermediate, and 14 adverse samples).

Hyperactive WNT Signaling Resulted Activated in Diffuse AC133^{bright} AML Cells Expressing the Hematopoietic Regenerative Molecule WNT10B

Most of what is known about hematopoietic regeneration point to WNT signaling pathway and specifically to *WNT10B* [13,45]; therefore,

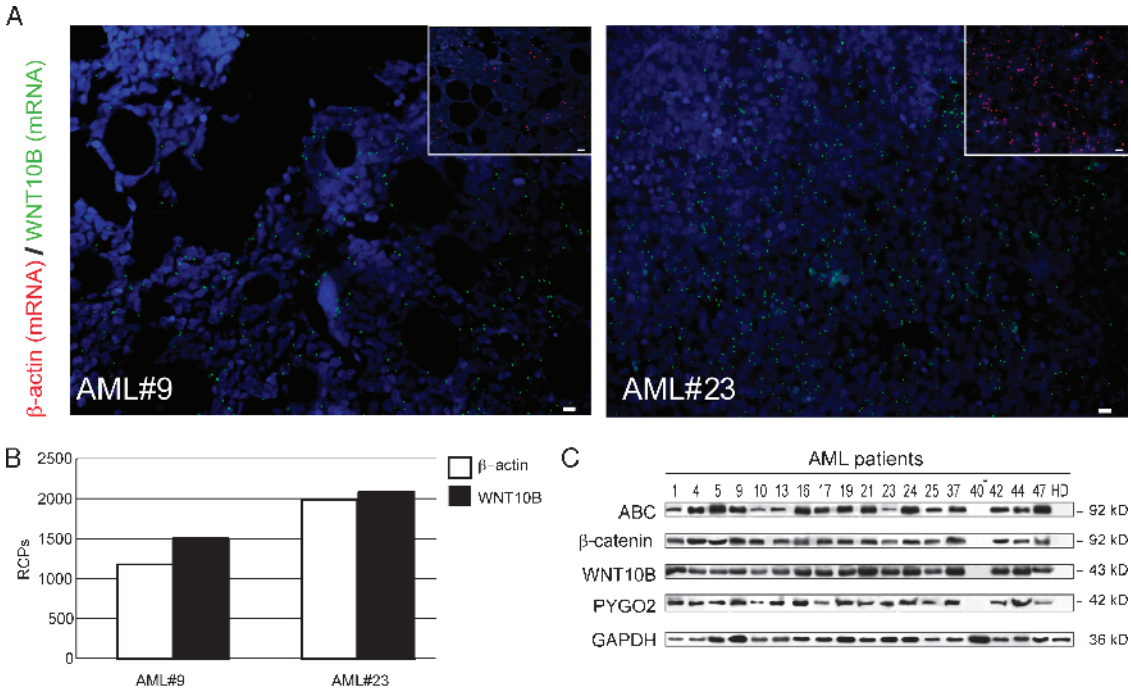

Figure 3. Altered WNT signaling in AC133$^+$ AML cells. (A) Detection with padlock probe and target-primed rolling circle amplification of individual *WNT10B* transcripts on BM slides from AML patients. Green RCPs represent *WNT10B* transcripts, and red RCPs represent β-actin transcripts in consecutive sections. Cell nuclei are shown in blue. Images were acquired with ×20 magnification. Scale bar, 10 μm. (B) The quantification of RCPs was done on three ×20 images of BM biopsies of AML patients. For quantification, the numbers of RCPs of each image were counted digitally using CellProfiler software. The average of RCPs for each sample was calculated and it is reported as a ratio between β-actin and WNT RCPs. (C) Immunoblot analysis of ABC, β-catenin (as detected with the N-terminal pan–β-catenin antibody), WNT10B, and Pygopus 2 protein expression in AC133$^+$ cell fractions from 18 patient samples and 1 healthy donor introduced as control. GAPDH, loading control. HD, healthy donor; *therapy-related secondary AML.

we investigated how expression of *WNT10B* is related to AML phenotype. To fully understand mRNA distribution of WNT10B within BM sections, we focused on the application of single molecule detection methods. *In situ* mRNA detection by target-primed rolling circle amplification analysis offers high sensitivity and localized detection within single cells and tissues [15]. Following this approach, we detected *WNT10B*-related transcript in BM sections obtained at diagnosis from two randomly selected patients. *β-Actin* was included as a reference transcript in consecutive sections. Visualization by using high-performance fluorescence microscopy showed a diffuse localization pattern in the tissues (Figure 3*A*). Signal distribution and RCP quantification showed a *β-actin/WNT10B* ratio close to 1, suggesting a constitutive activation of *WNT10B* transcription in the BM (Figure 3*B*). In addition, we analyzed transcriptional activation of canonical WNTs focusing on genes that have been shown to be potent regulators of stem cell functions. N-terminally dephosphorylated β-catenin (ABC) was increasingly accumulated as determined by immunoblot analysis (Figure 3*C*). Remarkably, we confirmed a dramatic increase in WNT10B expression in all patient samples, except for one, reanalyzed by immunoblot (Figure 3*C*). Interestingly, the only AML patient negative for the WNT10B expression (AML No. 40 in Table W1) was affected by therapy-related AML. According to the biologic relevance of PYGO2 in promoting the responsiveness of WNT signaling [35,36], diffuse overexpression was detected by immunoblot (Figure 3*C*). To better elucidate the impact of the broad WNT10B overexpression on the leukemic microenvironment, we examined its expression in histologic preparations of BM from five randomly selected AML patients at diagnosis. Double immunostaining for WNT10B and ABC, followed by ImageJ analysis, confirmed that WNT10B was expressed by a high proportion of leukemic cells. We next examined by immunostaining a number of BM biopsy sections from five randomly selected cases. In all the analyzed samples, the AC133 immunostaining revealed islands of highly positive cells ($AC133^{bright}$) in an estimated proportion of 8% of cells, amid $AC133^{dim}$ or negative tumor blasts (Figure 4*A*). $AC133^{bright}$ cells correlated with accumulation of ABC (Figure 4, *B* and *C*). WNT10B antibody staining was also detectable in interstitial spaces, suggesting its secretion and release in the BM microenvironment (Figure 4*D*, top). The slides revealed that WNT10B is diffusely expressed (Figure 4, *A* and *D*) but that only the $AC133^{bright}$ small cells (8–10 μm diameter of the nuclei), with a clonal appearance and increased N/C ratio, shared the WNT signaling activation signature represented by accumulation of ABC [46], likely induced through an autocrine/paracrine mechanism (Figure 4, *B* and *D*, top).

$AC133^+$ Leukemic Cells Express and Secrete WNT10B in a Primary Cell Culture

The notion that primary cell cultures closely mimic the *in vivo* state and generate more physiologically relevant data led us to establish a primary $AC133^+$ cell culture (A46). A46 cells, with diploid karyotype, were selected from a 66-year-old male at diagnosis of AML-M2 (AML No. 46 in Table W1). Immunophenotype of MNCs before selection revealed a dominant $CD133.1^+CD34^+CD38^-CD45^+CD117^+$ blast population (59%; Figure 5*A*), representing an optimal source to establish an LIC-enriched primary culture. Recently published data implicate the existence of an immunophenotypic hierarchy in AML, with a minority of $CD38^-CD45^+$ cells giving rise to $CD38^+CD45^+$ "GMP-like" cells at the apex of an LIC hierarchy [10]. The latter finding seems to suggest that $CD38^-CD45^+$ cells start to gain CD38 expression after AC133 selection procedures as observed in sorted cells (Figure 5*A*). Comparative analysis of spotted AC133-selected A46 leukemic and normal cells by

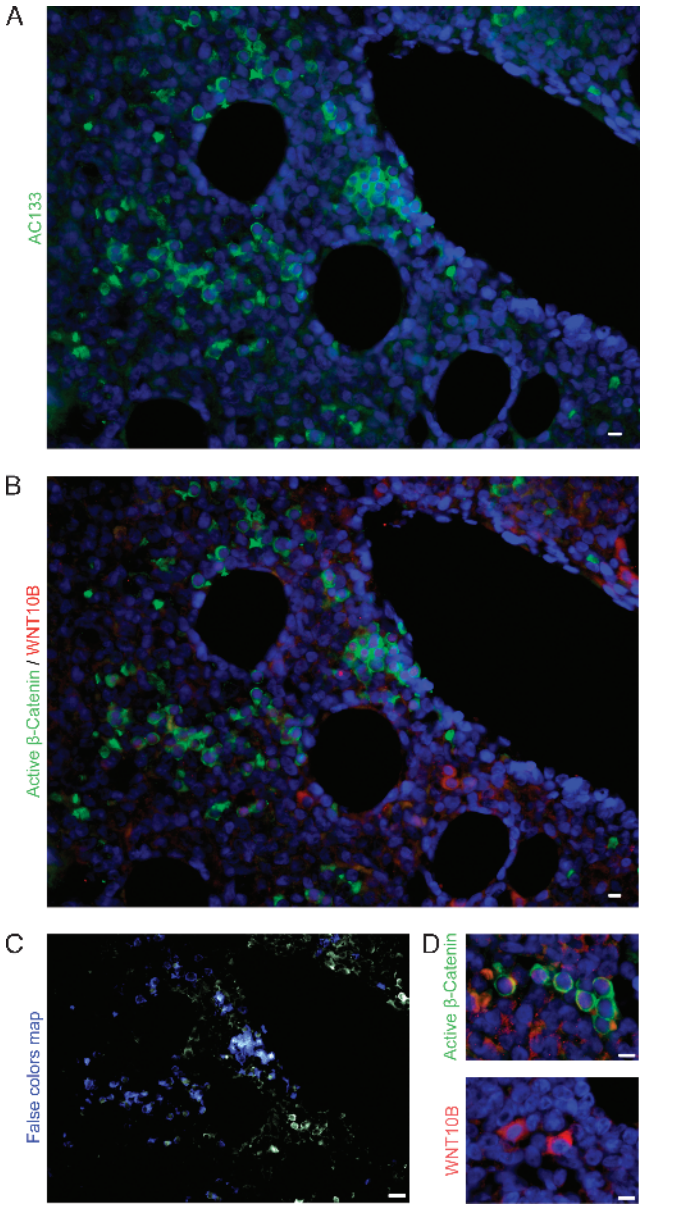

Figure 4. β-Catenin activation in the subpopulation of $AC133^{bright}$ AML cells expressing WNT10B. (A) Representative immunostaining micrographs show green fluorescence of cells expressing AC133 in a BM section of AML No. 9 (Table W1). Cell nuclei are shown in blue. Scale bar represents 10 μm. (B) Co-staining of BM from AML No. 9 adjacent serial section for expression of ABC (green) and WNT10B (red). Cell nuclei are shown in blue (DAPI). (C) False color maps of ABC/WNT10B double positive cells (blue) were obtained using an automatic threshold based on the moments algorithm implemented in the ImageJ program. DAPI staining was used to identify nuclei. Images obtained crossing ABC masks with WNT10B signals were used to count the percentage of ABC/WNT10B double positive cells over the total number of cells. The macro was validated against a trained experimenter over a sample of 830 total cells from eight different images. Differences in results were restricted to less than 0.01%. (D) Morphologic detail of cells showing intense specific staining for ABC (top panels) and WNT10B (bottom panels). All images were acquired with a ×40 objective. Scale bars represent 10 μm. Representative images of at least three serial slides from five randomly selected patients.

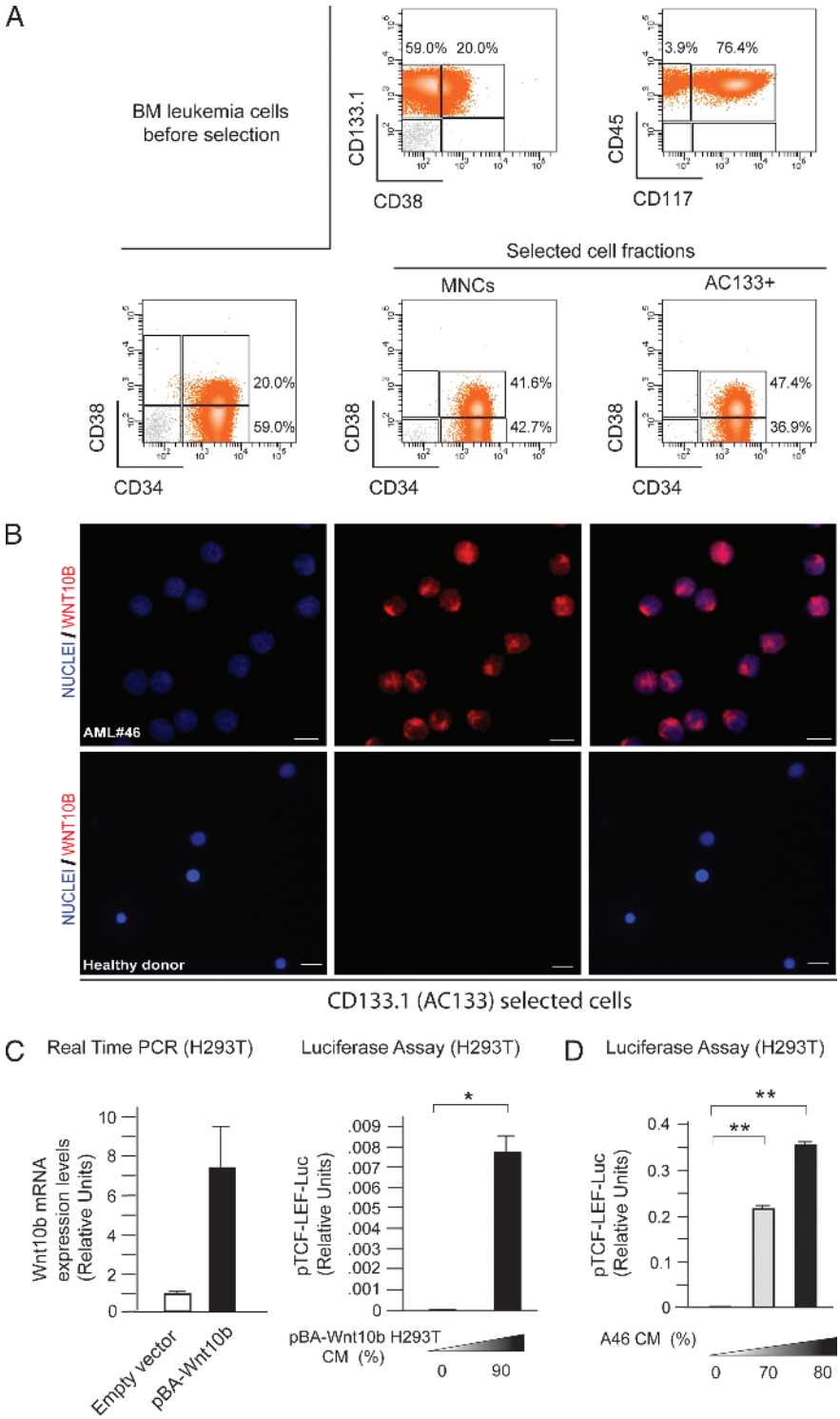

Figure 5. AC133$^+$ A46 cells express and release WNT10B. Dot plots of the immunophenotype analysis from AML No. 46 BM MNCs at diagnosis and after selection. (A) Patterns of CD38/CD133.1 (top left), CD117/CD45 (top right), and CD34/CD38 (bottom left) co-staining were gated on BM AML cells before selection. Representative CD34 and CD38 expression on Ficoll-selected MNCs (bottom center) and AC133-sorted cells before culture (bottom right) is shown. Percentages on total cellularity are shown for gated AML populations. (B) Immunostaining assessment for WNT10B in AC133$^+$ populations from A46 (top panels) or healthy donor (bottom panels). Representative images of at least five serial slides. Blue, nuclei; red, WNT10B; merge, WNT10B/DAPI. All images were acquired with a ×40 objective. Scale bars represent 10 μm. (C and D) TOPFlash reporter assay showing luciferase expression driven by eight TCF/lymphoid-enhancing factor (LEF) binding sites. (C) Positive control was obtained by CM of pBA-*WNT10B*–transfected H293T cells. Expression of *WNT10B* was evaluated in pBA-*WNT10B*–transfected H293T by real-time PCR (left). TOPFlash reporter assay shows luciferase expression induced in Super 8x TOPFlash–H293T cells by pBA–*WNT10B* H293T CM (right). (D) TOPFlash reporter assay showing dose-dependent luciferase expression induced in Super 8x TOPFlash–H293T cells by A46 CM. Significance was evaluated by the unpaired Student's *t* test: $*P < .05$; $**P < .001$. Data represent the mean ± SD of triplicate reactions and are representative of three independent experiments.

immunostaining revealed WNT10B expression in all A46 AC133$^+$ cells (Figure 5*B*, top), whereas normal BM-derived AC133$^+$ cells resulted negative (Figure 5*B*, bottom). To further investigate whether the endogenous WNT production had any paracrine effect, we used A46 CM to evaluate β-catenin–mediated transcriptional activation. To this aim, HEK293T cells (H293T), transfected with Super 8x TOPFlash β-catenin/TCF transcription–based reporter construct, were exposed either to pBA–*WNT10B* H293T CM as control (Figure 5*C*) or A46 CM. This construct could be efficiently expressed in a dose-dependent manner when transiently exposed to A46 CM for 12 hours (Figure 5*D*).

AC133 Is Expressed on Functional A46 AML LSC

To complement the *in vitro* observations, we tested whether AC133 was expressed on functional A46 AML LSC. We transplanted A46 cells into sublethally irradiated (5 Gy) 6-week-old Rag2$^{-/-}\gamma c^{-/-}$ mice via the tail vein. This highly immunodeficient mouse strain lacks mature B, T, and natural killer (NK) cells, supporting efficient engraftment of human AML [16]. Transplanted mice were killed at 3 to 8 weeks after transplantation and analyzed for engraftment of human leukemia cells in BM (Figure 6*A*). The results of a typical experiment from three transplanted mice (M1–M3) are shown in Figure 6, with AC133$^+$ A46 cells showing engraftment of human CD45 (hCD45) cells. We confirmed that engrafted hCD45$^+$ cells were human myeloid leukemia blasts by measuring CD34/CD38/CD133 expression (Figure 6*B*).

Transplantation of A46 Induces Ectopic Axial Structure Formation in Zebrafish Embryo by WNT Signaling Activation

To bring our functional analyses full circle, we explored the physiological relevance of tumor-derived WNT signals by using the developing zebrafish as a biosensor. We hypothesized that WNT-secreting A46 cells transplanted into developing zebrafish embryos might act as

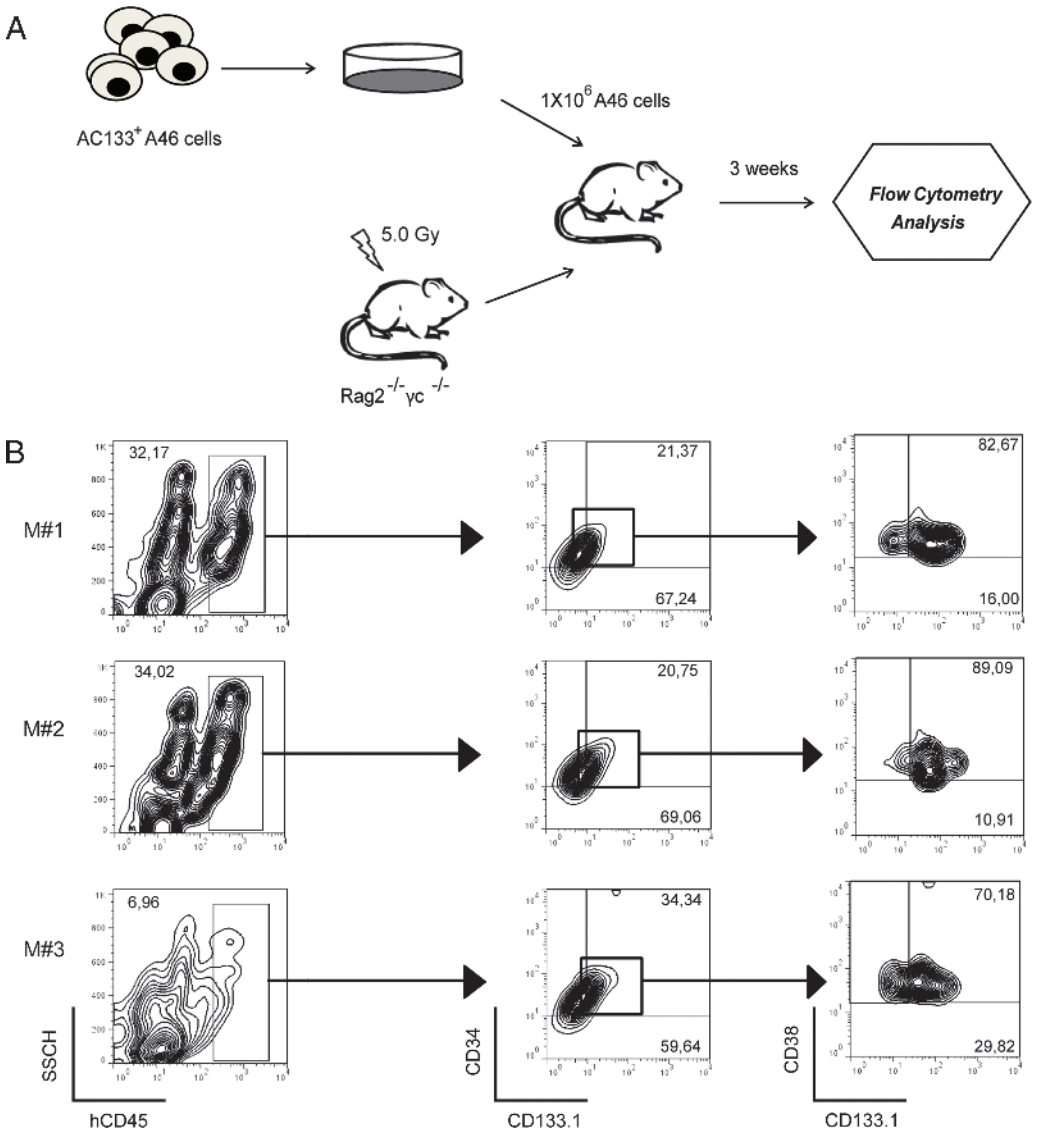

Figure 6. AC133$^+$ A46 cell transplantation in Rag2$^{-/-}\gamma c^{-/-}$ mice. (A) Overview of the experimental design: 1×10^6 AC133$^+$ A46 cells were injected into sublethally irradiated Rag2$^{-/-}\gamma c^{-/-}$ mice through the tail vein. Three weeks after transplantation, BM cells were collected and analyzed by flow cytometry. (B) Expression profiles of three recipient mice (M1–M3) are shown. hCD45$^+$ population was identified in BMs of mice, and within hCD45$^+$, the expression patterns of hCD34 and hCD133.1 (AC133) were analyzed. Cells were separated in subpopulations according to the expression of hCD34 and hCD133.1 and then analyzed for hCD38 and hCD133.1 expressions.

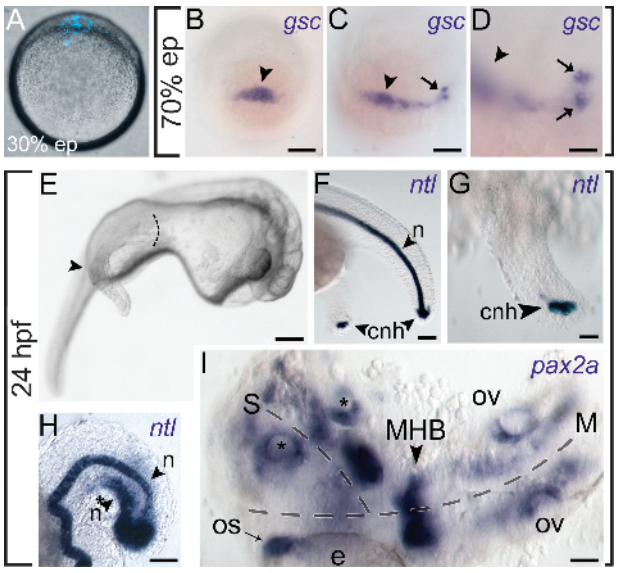

Figure 7. A46 AML cells induce ectopic gene expression and secondary body axis formation upon transplantation in zebrafish embryos. (A) Fluorescence microscopy of a live zebrafish embryo at 30% of epiboly (lateral view) transplanted at 3 hpf at the animal pole region with A46 cells previously blue-stained with Hoechst 33342. (B–D) Dorsal side view of 70% epiboly-stage embryos hybridized with a *gsc*-specific probe. Embryos have been injected with (B) normal AC133$^+$ cells as control or (C and D) A46 AML cells. The arrowheads indicate the *gsc* endogenous signal, while arrows specify the position of zebrafish cells expressing ectopic *gsc*. (E) Bright-field microscopy of a 24-hpf zebrafish embryo injected with A46 AML cells (lateral view). The arrowhead and the dotted line indicate the secondary trunk/tail induced by A46 cells. (F, G) The embryo in E has been hybridized with a probe specific for the notochord and tail bud marker *ntl*. (F) The probe labels the notochord (n) in the endogenous trunk and the chordoneural hinge (cnh) in both tails (G, higher magnification). (H) Tail of a 24-hpf embryo hybridized with *ntl*-specific probe. The endogenous (n) and ectopic (*n) *ntl* signals run parallel along the axis of the embryo, indicating the presence of additional axial structures. (I) Dorsal view of a 24-hpf embryo that developed an ectopic head on the side of the endogenous one, as indicated by the expression of the brain marker gene *pax2a*. The dotted lines indicate the main (M) and secondary (S) axes. The optic stalk (OS) in close vicinity to the eye (e), the midbrain-hindbrain boundary (MHB), and the otic vesicles (OV) of the embryo are stained with the *pax2a* riboprobe, as well as several areas of the ectopic head (the asterisks indicate the two clearly recognizable additional otic vesicles). The image is composed of different pictures corresponding to several focal planes, since the embryo is not flat, and a single focal plane cannot comprise all the labeled structures belonging to the main and secondary axes. Scale bars represent 125 μm (A–D), 150 μm (E), 40 μm (F), 15 μm (G and I), or 25 μm (H).

ectopic sources of maternal WNT ligands. Cell-grafted embryos, injected at or before the mid-blastula transition stage (~3 hpf) with Hoechst 33342 fluorescently labeled A46 cells (Figure 7*A*), showed the expression of the organizer-specific gene *goosecoid* (*gsc*). Expression of *gsc* is typically initiated by the nuclear translocation of maternal β-catenin triggered by the activation of the WNT signaling. While normal AC133$^+$ cells did not alter the normal expression of the gene (Figure 7*B*), approximately 30% of the embryos grafted with A46 cells (n = 208) displayed both the expansion of the *gsc* endogenous domain and the activation of the gene in ectopic positions (Figure 7, *C* and *D*). Consistent with our hypothesis, the A46 cells retain a dorsal organizer–inducing activity possibly correlated with their strong WNT signaling activation. In addition, grafted embryos developed secondary axial structures, ranging from additional tail tissues (Figure 7, *E–H*) to an almost fully formed ectopic head (Figure 7*I*). Control embryos grafted with normal BM-derived AC133$^+$ cells, devoid of any WNT signaling activity, did not display alterations of the normal phenotype (data not shown). The identity of the additional tail structures was confirmed by *in situ* hybridization staining for the notochord and tail bud marker *ntl* [47], whereas the emergence of ectopic head structures was highlighted by *pax2a* labeling optic stalk, midbrain–hindbrain boundary, and otic vesicles. These results imply that A46 cells might determine the establishment of an additional source of signal, with a Nieuwkoop center–like activity, able to induce an extra dorsal organizer, similarly to the endogenous situation at mid-blastula transition, when maternal WNT/β-catenin signaling initiates the formation of the dorsal organizer [48]. In zebrafish, secondary axis can be also induced by Nodal, a highly evolutionarily conserved morphogen belonging to the transforming growth factor–β superfamily and able to activate *gsc* expression [49]. Therefore, we investigated the possible involvement of the Nodal signaling pathway in the dorsal organizer induction mediated by A46 cells. The complete lack of *Nodal* expression observed after microarray analyses was confirmed by qualitative RT-PCR in A46 and samples from six different AML patients (Figure W1), allowing to exclude any *Nodal* contribution from A46 cells to the formation of the secondary axis and induction of *gsc* expression.

Discussion

The deceivingly homogeneous, undifferentiated morphology of the AML blasts is now known to mask a heterogeneous collection of cells that recapitulate the hierarchy of precursor cells that characterize the normal process of blood-cell differentiation. The concept that LIC properties occur in a self-renewing non-HSC progenitor cell population, preceded by the expansion of a preleukemic LT-HSC, has been recently reinforced [4,10]. However, the molecular functions responsible for the preleukemic LT-HSC expansion and the acquisition of self-renewal ability in AML remained poorly defined.

The WNT/β-catenin pathway has been show to play a critical role in the regulation of cell proliferation, differentiation, and apoptosis of different malignant entities. It is highly regulated in AML [50] and also involved in the self-renewal process of HSCs. WNT/β-catenin pathway requirement for LIC development in AML has emerged in mouse model [21]. Recent studies revealed aberrant WNT signaling in AML cells that is independent from the occurrence of AML-associated fusion proteins or mutations in tyrosine kinase receptors [reviewed in 20].

The results presented here using gene expression microarrays and pathway analysis provide direct evidence that the WNT/β-catenin signaling is diffusely activated in the AC133$^+$ AML population, with a specific transcriptional signature involving overexpression of the WNT pathway agonists and down-modulation of the major antagonists.

Although the long-term reconstituting human HSC marker AC133 has been detected in a majority of CD34$^+$ AML [51], no extensive data concerning the role of AC133 in AML were available.

Analysis of freshly fractionated cells from AML patients showed that active WNT signaling was predominant in the population highly enriched for the AC133 marker. Notably, *WNT2B*, *WNT6*, *WNT10A*, and *WNT10B*, known to promote hematopoietic tissue regeneration [13,14], are the WNT mediators specifically upregulated in the AC133$^+$

AML cells. In addition, there is evidence that in the hematopoietic system *WNT10B* is specifically and significantly upregulated following an injury and that WNT10B acts to enhance the growth of HSCs [13]. It is also worth noting that greater fold expansion of murine HSC progenitors was obtained after WNT10B CM exposure [52]. Consistent with the latter observations, we showed a dramatic increase of WNT10B expression and protein release within the microenvironment in the large majority of samples from AML patients recruited to this study, with the exception of the unique therapy-related AML patient. In accordance with previous reports [52], we have not detected *WNT10B* gene expression in normal AC133$^+$ hematopoietic cells. Moreover, our data also point to the strong expression of the WNT target gene *CD44* and the loss of *CD24*, according to the expression of CD44$^+$CD24$^-$AC133$^+$ phenotype that defines a putative cancer stem cell population also in breast tumors [53]. Interestingly, Dick et al. have shown that CD44 is a key regulator of AML LSC function and that targeting it eradicates LSCs [54]. In light of the higher homeostatic range of WNT/β-catenin signaling occurring upon an acute injury [55], our study demonstrated the involvement of the regeneration-associated WNT signaling in AC133^{bright} AML cell fraction. The term "regeneration" has been used to define the physiological phenomena of reconstitution from damage due to injury or disease. Hematopoietic regenerative-associated WNT ligand (WNT10B) is expressed at mRNA and protein levels on both leukemic blasts and stromal-like cells, indicating a possible autocrine/paracrine involvement of WNT in the BM microenvironment. Conversely, activation of WNT signaling marked by expression of the dephosphorylated β-catenin was restricted to the smaller population of AC133^{bright} leukemic cells. The reasons for these differences are unclear, but it is possible that β-catenin activation by WNTs requires the expression of specific Fzd receptors, conferring a "responsive" phenotype, only restricted to a rare population of cells. In the HSC biology, a fundamental question is how self-renewal is controlled; several lines of evidence point to Notch for a WNT-mediated maintenance of undifferentiated HSCs [56]. Recent studies, examining the molecular targets of WNT10B, have highlighted the nuclear factor κB and Notch pathways as downstream targets of WNT10B [57]. It is tempting to speculate that WNT10B and other regeneration-associated WNTs (i.e., WNT2B, WNT6, and WNT10A) integrate with other signals, such as Notch, to drive oncogenic renewal. Because activation of WNT signaling can increase the ability of HSCs to reconstitute the hematopoietic system of lethally irradiated mice, we transplanted the AC133$^+$ A46 cells into irradiated Rag2$^{-/-}\gamma c^{-/-}$ mice. Different papers have been recently published in which comparisons in the engraftment ability of different immunodeficient murine models were made. The variability of the reconstitution seemed to be mainly linked to the degree of immunodepression of the murine host. Rag2$^{-/-}\gamma c^{-/-}$ represents a powerful model to verify the biologic and malignant characteristics of human tumor cells. It is characterized by immunodeficiency of T and B cells caused by Rag2 knockout, coupled with the NK deficit mediated by the absence of the γc interleukin receptor chain [16]. The results of our experiments indicate that AC133 is expressed on AML LSC in the A46 primary cells, suggesting that regeneration-associated WNT expression signature is enriched in primary human AML LSC–containing fraction.

Regeneration requires the rapid expansions of HSCs; this process is often mediated by reactivation of developmental signal transduction pathways, such as BMP and WNT [45,58]. In the early embryo, the WNT factors induce the nuclear translocation of β-catenin, which triggers the formation of the dorsal organizer through the activation of zygotic dorsal-specific genes [59]. Such WNT-induced cascade of events results in the establishment of the embryonic dorsoventral axis [47]. To test the hypothesis that regeneration-associated WNT signaling is involved in AML LSC expansion, we used a zebrafish embryonic model as a tool by examining the ability of A46 primary leukemia cells to modulate embryonic microenvironment. Therefore, we used zebrafish embryos to show that A46 cells prompt secondary axis development, inducing the formation of a dorsal organizer–like structure, possibly through the secretion of different WNT ligands. The mechanisms promoting organizer formation are known to involve cooperation between Nodal and WNT signaling. However, implanted cell lines with different origin induce the dorsal organizer independently from the Nodal signaling [60]. Here, we demonstrated that the A46-dependent alteration of zebrafish development and activation of the organizer-specific gene *gsc* are not reliant on Nodal activity.

In summary, the findings we report here implicate, for the first time, that regeneration-associated ligand-dependent WNT signaling exceeds the homeostatic range in the majority of human AML cases and affects responsive AC133^{bright} cells whose renewal is promoted by WNT pathway activity *in vivo*. These results not only support that AC133 is expressed on functional leukemia stem cells, but because developmental signal transduction pathways are often reactivated during regeneration, we also show that AC133$^+$ AML cells induce the formation of a dorsal organizer–like structure in zebrafish embryos.

Finally, these studies suggest that the regenerative WNT signaling is a stem cell–associated function altered, as a common feature, in AC133^{bright} AML leukemia stem cell fraction. Future studies will be required to demonstrate a pathogenic association of AC133^{bright} LSC regeneration response with AML, in terms of tumorigenicity, clinicopathologic features, and patient outcomes.

Acknowledgments

We thank the patients with AML and their families. We also thank E. Cattaneo, G. Simonutti, R. Bacchetta, and N. Santo for support with microscopy facilities, U. Landegren and O. Soderberg for supporting our activities at Rudbeck Laboratory, B. Scarpati and E. Calzavara for assistance with flow cytometry, R. Brusamolino and L. Pezzetti for assistance with patients' samples, L. Prosperi for support with zebrafish procedures, and S. Pozzi for helpful discussion.

References

[1] Cozzio A, Passegué E, Ayton PM, Karsunky H, Cleary ML, and Weissman IL (2003). Similar MLL-associated leukemias arising from self-renewing stem cells and short-lived myeloid progenitors. *Genes Dev* **17**, 3029–3035.

[2] Somervaille TC, Matheny CJ, Spencer GJ, Iwasaki M, Rinn JL, Witten DM, Chang HY, Shurtleff SA, Downing JR, and Cleary ML (2006). Hierarchical maintenance of MLL myeloid leukemia stem cells employs a transcriptional program shared with embryonic rather than adult stem cells. *Cell Stem Cell* **4**, 129–140.

[3] Kirstetter P, Schuster MB, Bereshchenko O, Moore S, Dvinge H, Kurz E, Theilgaard-Mönch K, Månsson R, Pedersen TA, Pabst T, et al. (2008). Modeling of C/EBPα mutant acute myeloid leukemia reveals a common expression signature of committed myeloid leukemia-initiating cells. *Cancer Cell* **13**, 299–310.

[4] Bereshchenko O, Mancini E, Moore S, Bilbao D, Månsson R, Luc S, Grover A, Jacobsen SE, Bryder D, and Nerlov C (2009). Hematopoietic stem cell expansion precedes the generation of committed myeloid leukemia-initiating cells in C/EBPα mutant AML. *Cancer Cell* **16**, 390–400.

[5] Beachy PA, Karhadkar SS, and Berman DM (2004). Tissue repair and stem cell renewal in carcinogenesis. *Nature* **432**, 324–331.

[6] Goessling W, North TE, Loewer S, Lord AM, Lee S, Stoick-Cooper CL, Weidinger G, Puder M, Daley GQ, Moon RT, et al. (2009). Genetic interaction of PGE2 and Wnt signaling regulates developmental specification of stem cells and regeneration. *Cell* **136**, 1136–1147.

[7] Zhao C, Chen A, Jamieson CH, Fereshteh M, Abrahamsson A, Blum J, Kwon HY, Kim J, Chute JP, Rizzieri D, et al. (2009). Hedgehog signalling is essential for maintenance of cancer stem cells in myeloid leukaemia. *Nature* **458**, 776–779.

[8] Hofmann I, Stover EH, Cullen DE, Mao J, Morgan KJ, Lee BH, Kharas MG, Miller PG, Cornejo MG, Okabe R, et al. (2009). Hedgehog signaling is dispensable for adult murine hematopoietic stem cell function and hematopoiesis. *Cell Stem Cell* **4**, 559–567.

[9] Taussig DC, Miraki-Moud F, Anjos-Afonso F, Pearce DJ, Allen K, Ridler C, Lillington D, Oakervee H, Cavenagh J, Agrawal SG, et al. (2008). Anti-CD38 antibody-mediated clearance of human repopulating cells masks the heterogeneity of leukemia-initiating cells. *Blood* **112**, 568–575.

[10] Goardon N, Marchi E, Atzberger A, Quek L, Schuh A, Soneji S, Woll P, Mead A, Alford KA, Rout R, et al. (2011). Coexistence of LMPP-like and GMP-like leukemia stem cells in acute myeloid leukemia. *Cancer Cell* **19**, 138–152.

[11] Yin AH, Miraglia S, Zanjani ED, Almeida-Porada G, Ogawa M, Leary AG, Olweus J, Kearney J, and Buck DW (1997). AC133, a novel marker for human hematopoietic stem and progenitor cells. *Blood* **90**, 5002–5012.

[12] Mizrak D, Brittan M, and Alison MR (2007). CD133: molecule of the moment. *J Pathol* **214**, 3–9.

[13] Congdon KL, Voermans C, Ferguson EC, DiMascio LN, Uqoezwa M, Zhao C, and Reya T (2008). Activation of Wnt signaling in hematopoietic regeneration. *Stem Cells* **26**, 1202–1210.

[14] Katoh M and Katoh M (2006). Cross-talk of WNT and FGF signaling pathways at GSK3β to regulate β-catenin and SNAIL signaling cascades. *Cancer Biol Ther* **5**, 1059–1064.

[15] Larsson C, Grundberg I, Söderberg O, and Nilsson M (2010). *In situ* detection and genotyping of individual mRNA molecules. *Nat Methods* **7**, 395–397.

[16] Shinkai Y, Rathbun G, Lam KP, Oltz EM, Stewart V, Mendelsohn M, Charron J, Datta M, Young F, Stall AM, et al. (1992). RAG-2-deficient mice lack mature lymphocytes owing to inability to initiate V(D)J rearrangement. *Cell* **68**, 855–867.

[17] Majeti R, Becker MW, Tian Q, Lee TL, Yan X, Liu R, Chiang JH, Hood L, Clarke MF, and Weissman IL (2009). Dysregulated gene expression networks in human acute myelogenous leukemia stem cells. *Proc Natl Acad Sci USA* **106**, 3396–3401.

[18] Reya T, Duncan AW, Ailles L, Domen J, Scherer DC, Willert K, Hintz L, Nusse R, and Weissman IL (2003). A role for Wnt signalling in self-renewal of haematopoietic stem cells. *Nature* **423**, 409–414.

[19] Staal FJT and Luis TC (2010). Wnt signaling in hematopoiesis: crucial factors for self-renewal, proliferation, and cell fate decisions. *J Cell Biochem* **109**, 844–849.

[20] Mikesch JH, Steffen B, Berdel WE, Serve H, and Müller-Tidow C (2007). The emerging role of Wnt signaling in the pathogenesis of acute myeloid leukemia. *Leukemia* **21**, 1638–1647.

[21] Wang Y, Krivtsov AV, Sinha AU, North TE, Goessling W, Feng Z, Zon LI, and Armstrong SA (2010). The Wnt/β-catenin pathway is required for the development of leukemia stem cells in AML. *Science* **327**, 1650–1653.

[22] Scheller M, Huelsken J, Rosenbauer F, Taketo MM, Birchmeier W, Tenen DG, and Leutz A (2006). Hematopoietic stem cell and multilineage defects generated by constitutive β-catenin activation. *Nat Immunol* **7**, 1037–1047.

[23] Kirstetter P, Anderson K, Porse BT, Jacobsen SE, and Nerlov C (2006). Activation of the canonical Wnt pathway leads to loss of hematopoietic stem cell repopulation and multilineage differentiation block. *Nat Immunol* **7**, 1048–1056.

[24] Smith ML, Hills RK, and Grimwade D (2011). Independent prognostic variables in acute myeloid leukaemia. *Blood Rev* **25**, 39–51.

[25] Brioschi M, Fischer J, Cairoli R, Rossetti S, Pezzetti L, Nichelatti M, Turrini M, Corlazzoli F, Scarpati B, Morra E, et al. (2010). Down-regulation of microRNAs 222/221 in acute myelogenous leukemia with deranged core-binding factor subunits. *Neoplasia* **12**, 866–876.

[26] Falcon S and Gentleman R (2007). Using GOstats to test gene lists for GO term association. *Bioinformatics* **23**(2), 257–258.

[27] Huang DW, Sherman BT, and Lempicki RA (2009). Systematic and integrative analysis of large gene lists using DAVID bioinformatics resources. *Nat Protoc* **4** (1), 55–57.

[28] Hatta K and Takahashi Y (1996). Secondary axis induction by heterospecific organizers in zebrafish. *Dev Dyn* **205**, 183–195.

[29] Thisse C, Thisse B, Schilling TF, and Postlethwait JH (1993). Structure of the zebrafish *snail1* gene and its expression in wild-type, *spadetail* and *no tail* mutant embryos. *Development* **119**, 1203–1215.

[30] Hess DA, Wirthlin L, Craft TP, Herrbrich PE, Hohm SA, Lahey R, Eades WC, Creer MH, and Nolta JA (2006). Selection based on CD133 and high aldehyde dehydrogenase activity isolates long-term reconstituting human hematopoietic stem cells. *Blood* **107**, 2162–2169.

[31] Hamamoto R, Silva FP, Tsuge M, Nishidate T, Katagiri T, Nakamura Y, and Furukawa Y (2006). Enhanced SMYD3 expression is essential for the growth of breast cancer cells. *Cancer Sci* **97**, 113–118.

[32] Mao B and Niehrs C (2003). Kremen2 modulates Dickkopf2 activity during Wnt/LRP6 signaling. *Gene* **302**, 179–183.

[33] Sinner D, Kordich JJ, Spence JR, Opoka R, Rankin S, Lin SC, Jonatan D, Zorn AM, and Wells JM (2007). Sox17 and Sox4 differentially regulate β-catenin/T-cell factor activity and proliferation of colon carcinoma cells. *Moll Cell Biol* **27**, 7802–7815.

[34] Olson LE, Tollkuhn J, Scafoglio C, Krones A, Zhang J, Ohgi KA, Wu W, Taketo MM, Kemler R, Grosschedl R, et al. (2006). Homeodomain-mediated β-catenin-dependent switching events dictate cell-lineage determination. *Cell* **125**, 593–605.

[35] Mieszczanek J, de la Roche M, and Bienz M (2008). A role of Pygopus as an anti-repressor in facilitating Wnt-dependent transcription. *Proc Natl Acad Sci USA* **105**, 19324–19329.

[36] Gu B, Sun P, Yuan Y, Moraes RC, Li A, Teng A, Agrawal A, Rhéaume C, Bilanchone V, Veltmaat JM, et al. (2009). Pygo2 expands mammary progenitor cells by facilitating histone H3 K4 methylation. *J Cell Biol* **185**, 811–826.

[37] Gehrke I, Gandhirajan RK, and Kreuzer KA (2009). Targeting the WNT/β-catenin/TCF/LEF1 axis in solid and haematological cancers: multiplicity of therapeutic options. *Eur J Cancer* **45**, 2759–2767.

[38] Angers S, Thorpe CJ, Biechele TL, Goldenberg SJ, Zheng N, MacCoss MJ, and Moon RT (2006). The KLHL12–Cullin-3 ubiquitin ligase negatively regulates the Wnt–β-catenin pathway by targeting Dishvelled for degradation. *Nat Cell Biol* **8**, 348–357.

[39] Li Y, Lu W, King TD, Liu CC, Bijur GN, and Bu G (2010). Dkk1 stabilizes Wnt co-receptor LRP6: implication for Wnt ligand-induced LRP6 down-regulation. *PloS One* **5**, e11014.

[40] Wang K, Zhang Y, Li X, Chen L, Wang H, Wu J, Zheng J, and Wu D (2008). Characterization of the Kremen-binding site on Dkk1 and elucidation of the role of Kremen in Dkk-mediated Wnt antagonism. *J Biol Chem* **22**, 23371–23375.

[41] Morris EJ, Ji JY, Yang F, Di Stefano L, Herr A, Moon NS, Kwon EJ, Haigis KM, Näär AM, and Dyson NJ (2008). E2F1 represses β-catenin transcription and is antagonized by both pRB and CDK8. *Nature* **25**, 552–556.

[42] Gao X, Wen J, Zhang L, Li X, Ning Y, Meng A, and Chen YG (2008). Dapper1 is a nucleocytoplasmic shuttling protein that negatively modulates Wnt signaling in the nucleus. *J Biol Chem* **283**, 35679–35688.

[43] Sampson EM, Haque ZK, Ku MC, Tevosian SG, Albanese C, Pestell RG, Paulson KE, and Yee AS (2001). Negative regulation of the Wnt–β-catenin pathway by the transcriptional repressor HBP1. *EMBO J* **20**, 4500–4511.

[44] Quéré R, Andradottir S, Brun AC, Zubarev RA, Karlsson G, Olsson K, Magnusson M, Cammenga J, and Karlsson S (2011). High levels of the adhesion molecule CD44 on leukemic cells generate acute myeloid leukemia relapse after withdrawal of the initial transforming event. *Leukemia* **25**, 515–526.

[45] Bowman TV, Tropouki E, and Zon LI (2012). Linking hematopoietic regeneration to developmental signaling pathways: a story of BMP and Wnt. *Cell Cycle* **11**, 424–425.

[46] Staal FJ, Noort Mv M, Strous GJ, and Clevers HC (2002). Wnt signals are transmitted through N-terminally dephosphorylated β-catenin. *EMBO Rep* **31**, 63–68.

[47] Lin X, Rinaldo L, Fazly AF, and Xu X (2007). Depletion of Med10 enhances Wnt and suppresses Nodal signaling during zebrafish embryogenesis. *Dev Biol* **303**, 536–548.

[48] Langdon YG and Mullins MC (2011). Maternal and zygotic control of zebrafish dorsoventral axial patterning. *Annu Rev Genet* **45**, 357–377.

[49] Schier AF (2003). Nodal signaling in vertebrate development. *Annu Rev Cell Dev Biol* **19**, 589–621.

[50] Siapati EK, Papadaki M, Kozaou Z, Rouka E, Michali E, Savvidou I, Gogos D, Kyriakou D, Anagnostopoulos NI, and Vassilopoulos G (2010). Proliferation and bone marrow engraftment of AML blasts is dependent on β-catenin signaling. *Br J Haematol* **152**, 164–174.

[51] Fauth F, Weidmann E, Martin H, Schneider B, Sonnhoff S, and Hoelzer D (2001). AC133 expression on acute myeloid leukemia blasts: correlation to FAB and to CD34 expression and possible implications for peripheral blood progenitor cell purging in AML. *Leuk Res* **25**(3), 191–196.

[52] Austin TW, Solar GP, Ziegler FC, Liem L, and Matthews W (1997). A role for the Wnt gene family in hematopoiesis: expansion of multilineage progenitor cells. *Blood* **89**, 3624–3635.

[53] Wright MH, Calcagno AM, Salcido CD, Carlson MD, Ambudkar SV, and Varticovski L (2008). *Brca1* breast tumors contain distinct CD44$^+$/CD24$^-$ and CD133$^+$ cells with cancer stem cell characteristics. *Breast Cancer Res* **10**, 1–16.

[54] Jin L, Hope KJ, Zhai Q, Smadja-Joffe F, and Dick JE (2006). Targeting of CD44 eradicates human acute myeloid leukemic stem cells. *Nat Med* **12**, 1167–1174.

[55] Angers S and Moon RT (2009). Proximal events in Wnt signal transduction. *Nat Rev Mol Cell Biol* **10**, 468–477.

[56] Duncan AW, Rattis FM, DiMascio LN, Congdon KL, Pazianos G, Zhao C, Yoon K, Cook JM, Willert K, Gaiano N, et al. (2005). Integration of Notch and Wnt signaling in hematopoietic stem cell maintenance. *Nat Immunol* **6**(3), 314–322.

[57] Mödder UI, Oursler MJ, Khosla S, and Monroe DG (2011). Wnt10b activates the Wnt, Notch and NFκB pathways in U2OS osteosarcoma cells. *J Cell Biochem* **112**(5), 1392–1402.

[58] Trompouki E, Bowman TV, Lawton LN, Fan ZP, Wu DC, DiBiase A, Martin CS, Cech JN, Sessa AK, Leblanc JL, et al. (2011). Lineage regulators direct BMP and WNT pathways to cell-specific programs during differentiation and regeneration. *Cell* **147**, 577–589.

[59] Lu FI, Thisse C, and Thisse B (2011). Identification and mechanism of regulation of the zebrafish dorsal determinant. *Proc Natl Acad Sci USA* **108**, 15876–15880.

[60] Hashiguchi M, Shinya M, Tokumoto M, and Sakai N (2008). Nodal/Bozozok-independent induction of the dorsal organizer by zebrafish cell lines. *Dev Biol* **321**, 387–396.

Table W1. Clinical Characteristics and Outcome of AML Patients.

No.	Age, y/Sex	FAB	Cytogenetics*	FLT3	NPM1	WBC, $\times 10^9$/L	MO Blast, %	EML	s-AML	Response to Induction	Relapse	Outcome
1	67/M	M2	45,XY,−7	wt	–	1.7	55	Absent	Yes†	CR	Yes	D/first res rel
2	45/M	M1	Complex karyotype	wt	–	1.7	60	Absent	No	CR	No	A/first CR
4	59/M	M4	46,XY,del(20)(q11;q13)	wt	–	3.5	32	Absent	No	CR	No	A/first CR
5	47/F	M4	46,XX	ITD	–	84.6	80	Skin	No	CR	No	A/first CR
6	76/F	M4	47,XX,+11	wt	–	–	–	Absent	Yes†	ref dis	n.a.	D/prim ref dis
9	20/M	M0	46,XY	wt	–	3.6	80	Absent	No	CR	Yes	A/second CR
10	62/F	M5a	46,XX	wt	–	69	90	Skin	No	CR	No	A/first CR
13	57/M	M1	46,XY,t(6;9)(p23;q34)	ITD	wt	39.7	89	Absent	No	ref dis	n.a.	D/prim ref dis
14	72/F	M2	46,XX	wt	–	–	–	Absent	No	ref dis	n.a.	D/prim ref dis
16	41/F	M2	46,XX	wt	wt	15.9	45	Absent	No	CR	No	A/first CR
17	29/M	M1	46,XY	ITD	wt	217.7	96	Absent	No	CR	Yes	D/first res rel
19	29/F	M1	46,XX,del(11)(q23)	wt	–	110.6	95	Skin	No	ref dis	Yes	D/first res rel
21	22/M	M1	46,XY	ITD	wt	16.7	75	Absent	No	CR	No	A/first CR
23	65/M	M1	46,XY	wt	wt	12.7	78	Absent	No	CR	Yes	A/second CR
24	59/M	M1	46,XY	wt	Exon 12	20.1	75	Absent	No	CR	Yes	A/first rel
25	39/F	M1	46,XX,del(11)(q23)	wt	wt	15.7	–	Absent	No	ref dis	n.a.	D/prim ref dis
30	41/M	M5a	46,XY	wt	wt	3.6	75	Absent	No	CR	Yes	A/first rel
32	52/F	M2	46,XX	wt	wt	2.7	55	Absent	Yes†	CR	No	D/TRM first CR
34	29/M	M0	46,XY,del(11)(q13;q23)	wt	wt	4	86	Absent	No	CR	Yes	D/first res rel
38	59/F	M1	46,XX	wt	Exon 12	1	82	Absent	No	CR	Yes	D/first res rel
39	51/M	n.a.	Complex karyotype	wt	wt	1.2	–	Absent	No	ref dis	n.a.	D/prim ref dis
40	55/F	M2	Complex karyotype	wt	wt	0.8	20	Absent	Yes‡	n.a.	n.a.	A/active dis
41	62/F	M4	46,XX	wt	wt	17	30	Skin	Yes†	CR	Yes	A/first res rel
42	65/F	M4	46,XX	wt	wt	1.2	60	Adnexal mass	No	ref dis	n.a.	A/prim ref dis
44	56/F	M2	46,XX,t(8;21)(q22;q22)	wt	wt	8.6	65	Absent	No	CR	Yes	A/second rel
46	66/M	M2	46,XY	ITD	wt	26.8	80	Absent	No	PR	n.a.	A/prim ref dis
47	62/F	M2	47,XX,+21	wt	Exon 12	23	12	Absent	Yes†	n.a.	n.a.	A/active dis
48	43/M	M5a	46,XY	ITD	Exon 12	63.9	85	Absent	No	CR	Yes	A/second CR
49	68/F	biphen.	45,XX,−7,t(9;22)(q34;q11)	wt	wt	8.1	70	Absent	No	CR	Yes	A/second CR
50	61/F	M4	Complex karyotype	wt	wt	8.8	35	Absent	No	ref dis	n.a.	D/prim ref dis
51	15/F	M5b	46,XX	wt	wt	118	84	CNS	No	CR	Yes	D/first res rel
52	33/M	M2	46,XY	wt	Exon 12	20.9	40	Absent	No	CR	No	A/first CR
53	51/F	M1	46,XX	wt	Exon 12	81.1	77	Absent	No	CR	No	A/first CR

A, alive; CR, complete remission; PR, partial remission; D, dead; ref dis, refractory disease; res rel, resistant relapse; biphen, biphenotypic; TRM, transplant-related mortality; s-AML, secondary AML; EML, extramedullary leukemia; n.a., not applicable.
*At diagnosis.
†Myelodysplastic AML.
‡Therapy-related AML.

Table W2. Top 10 Dysregulated KEGG Pathways in AC133$^+$ AML Cells.

Term	No. of Genes	*P*
Oxidative phosphorylation	78	9.9×10^{-7}
Focal adhesion	107	7.0×10^{-3}
Neurotrophin signaling pathway	70	7.3×10^{-3}
Ribosome	51	1.0×10^{-2}
Calcium signaling pathway	94	1.1×10^{-2}
Adherens junction	45	1.3×10^{-2}
Long-term potentiation	40	1.6×10^{-2}
Axon guidance	71	1.9×10^{-2}
WNT signaling pathway	80	2.2×10^{-2}
Ubiquitin-mediated proteolysis	73	2.3×10^{-3}

No. of genes is referred to KEGG pathway.
P is obtained through the modified Fisher exact test (EASE score in DAVID).

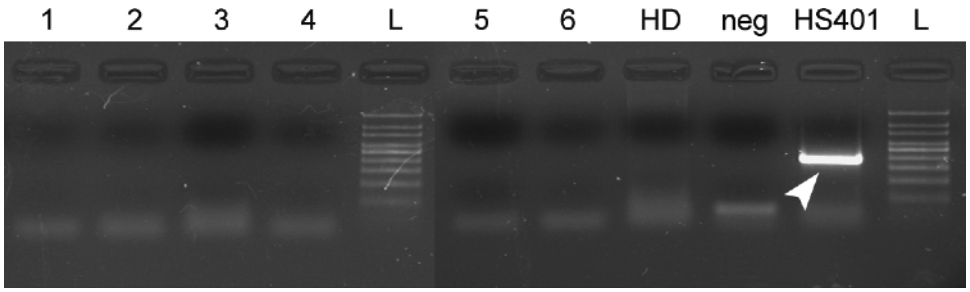

Figure W1. Nodal expression analysis on BM samples from AML patients. RT-PCR analysis has been performed to investigate the level of Nodal expression in AML samples from six different patients (lanes 1 to 6). The analysis has also been performed on BM specimen sampled from a healthy donor (lane HD), and monitored for quality with a positive control (lane HS401, human embryonic stem cell line HS401) and a no cDNA negative control (lane neg). A 100-bp molecular weight DNA ladder (Genespin) has been loaded onto the gel for amplicon sizing (lane L). The analysis pointed out the complete lack of *Nodal* expression in all the six samples tested, as well as, unsurprisingly, in the healthy donor. Arrowhead indicates the size of the Nodal-specific PCR product (392 bp) obtained with the following pair of primers: HuNODAL_ff2: 5′AGGGCGAGTGTCCTAATCCT and HuNODAL_rr: 5′CAGACTCCACTGAGCCCTTC. To further increase the sensitivity of the assay, we have subjected the PCRs to a second round of amplification using a semi-nested approach with the same reverse primer and with a nested forward primer (HuNODAL_ff1: 5′GAGGAGTTTCATCCGACCAA). The semi-nested PCR confirmed the total absence of *Nodal* expression in all the six samples analyzed, with the expected 366-bp product detected exclusively in the positive control (not shown, figure available upon request). To further increase the strength of the data, we have performed the same analysis on a second set of seven AML BM specimens, resulting in the exact same outcome (not shown, figure available upon request). GAPDH was used as internal control to test the good quality of all the cDNAs used in the experiments (not shown, figure available upon request).

Old and new prognostic factors in acute myeloid leukemia with deranged core-binding factor beta

Roberto Cairoli,[1,2] Alessandro Beghini,[3] Mauro Turrini,[1] Giambattista Bertani,[4] Gianpaolo Nadali,[5] Francesco Rodeghiero,[6] Carlo Castagnola,[7] Francesca Lazzaroni,[3] Michele Nichelatti,[1] Felicetto Ferrara,[8] Giovanni Pizzolo,[5] Enrico Pogliani,[9] Giuseppe Rossi,[10] Giovanni Martinelli,[11] and Enrica Morra[1]

[1] Division of Haematology, Niguarda Hospital, Milan, Italy

[2] Division of Haematology, Valduce Hospital, Como, Italy

[3] Department of Medical Biotechnology and Translational Medicine, University of Milan, Milan, Italy

[4] Division of Transfusion Medicine, Niguarda Hospital, Milan, Italy

[5] Department of Clinical and Experimental Medicine, University of Verona, Verona, Italy

[6] Department of Haematology, San Bortolo Hospital, Vicenza, Italy

[7] Department of Haematology Oncology, University of Pavia & Fondazione IRCCS Policlinico San Matteo, Pavia, Italy

[8] Division of Haematology and Stem Cell Transplantation Unit, Cardarelli General Hospital, Naples, Italy

[9] Division of Hematology and Bone Marrow Transplantation Unit, San Gerardo University Hospital, Monza, Italy

[10] Department of Haematology, Spedali Civili, Brescia, Italy; and [11] Division of Haematology and Stem Cell Transplantation Unit, Bologna, Italy

Corresponding Author:
Roberto Cairoli, MD
Department of Internal Medicine, Division of Haematology, Valduce Hospital
11, via Dante Alighieri
22100 Como, Italy
Tel: +39 031 324 111
Fax: +39 031 308 047
Email: rcairoli@valduce.it

Running Title: Prognostic factors in CBF-beta AML

Word Count: 3,725

ABSTRACT

Acute myeloid leukemia (AML) with deranged core-binding factor beta (CBFβ) is usually associated with a favourable prognosis with 50–70% of patients cured using contemporary treatments. We analyzed the prognostic significance of clinical features on 58 patients with CBFβ-AML aged ≤60 years. Increasing age was the only predictor for survival (*P*<0.001), with an optimal cut-point at 43 years. White blood cells (WBC) at diagnosis emerged as an independent risk factor for relapse incidence (*P*=0.017), with 1.1% increase of hazard for each $1.0x10^9$/L WBC increment. *KIT* mutations lacked prognostic value for survival and showed only a trend for relapse incidence (*P*=0.069).

Keywords

acute myeloid leukemia, core-binding factor, *KIT*, age, prognosis

1. Introduction

Among acute myeloid leukemias (AML) with recurrent genetic abnormalities, patients with t(8;21)(q22;q22), inv(16)(p13q22) or t(16;16)(p13;q22), are referred to as core binding factor (CBF)-AML. Although CBF-AML patients share a common molecular pathogenetic event, nominally the creation of a fusion protein involving a CBF gene unit, these two types of AML differ with regard to morphologic presentation, immunophenotypic marker expression, prognostic factors and response to treatments, and should be considered as distinct clinical entities [1,2].

In the inv(16)/t(16;16) group, the CBF-beta (CBFβ) gene located on 16q22 fuses to the MYH11 gene on 16p13, resulting in a chimeric protein. The translocation t(16;16)(p13;q22) is an equivalent rearrangement with lower incidence. Cytogenetically, the CBFβ-MYH11 rearrangement may be associated with trisomies of the chromosomes 8, 21, and 22 or with deletion of the chromosome 7 [3,4]. Patients with CBFβ-AML account for about 5-8% of adults with de novo AML and they are frequently associated with specific characteristics. This AML subset is morphologically associated with the French-American-British (FAB) M4 subtype with an abnormal eosinophil component (M4eo) and extramedullary involvement may be present [3-9].

Clinically, patients with CBFβ-AML are closely associated with a favourable outcome as compared with other AML subtypes [10-15]. High complete remission (CR) rate and prolonged disease-free survival may be achieved when patients are treated with standard induction therapy followed by high-dose cytarabine (HD-AraC) post-remission therapies [16]. Despite these results, the outcome of CBFβ-AML patients does not appear to be as homogeneous as their cytogenetic definition, since only 54 to 74% are cured using contemporary treatment [17]. Recurrent disease occurs in 30–40% of patients, with a significant number of them subsequently dying from disease progression. Prognostic factors of relapse risk in CBFβ-AML subset are still a matter of debate. Female gender, older age and low platelet count have been reported as predictors for inferior outcome and/or shorter disease-free survival in patients enrolled in prospective trials [1,17,18]. Furthermore, higher white blood cells (WBC) and low platelet counts have been identified as bad predictor factors for CR achievements [19,20]. Conversely, non-random additional cytogenetic abnormalities such as trisomy +22, and male sex predicted better outcome [1,21].

Gene mutations represent novel prognostic markers in CBFβ-AML. The most common gene mutations in the inv(16)/t(16;16) group are those involving the *KIT* gene, that are observed approximately in 20% to 30% of patients [22-24]. Retrospective studies have demonstrated that the presence of *KIT* mutations in exon 17 have been associated with a poor outcome in CBF-AML and, for that reason, *KIT* mutation testing has been recently incorporated into National Cancer Guidelines to better stratify such patients in different prognostic subgroups [25]. However, while several studies showed that activating *KIT* mutations confer a significantly lower survival in AML with t(8;21)(q22;q22), the negative prognostic impact of *KIT* mutations in CBFβ-AML remains controversial [24,26-33].

In this study, we analyze the prognostic significance of clinical and genetic features such as age, gender, WBC count, presence of extramedullary leukemia (EML), additional cytogenetic abnormalities and *KIT* mutations on long-term outcome of a large group of adult patients with inv(16)/t(16;16). Our results indicate that increasing age is the best predictor for survival of CBFβ-AML patients aged less than or equal to 60 years at univariate and multivariate analysis. Interestingly, *KIT* mutations lack prognostic value in term of

both survival and relapse incidence. This result contrasts with the observation done in AML with t(8;21)(q22;q22), suggesting differences in biology of CBF-AMLs.

2. Design and Methods

2.1. Patients' characteristics, data collection and treatment protocols

Fifty-eight patients aged less than or equal to 60 years with untreated AML presenting inv(16)(p13q22) or t(16;16)(p13;q22) diagnosed in 8 Italian centres were included in this study (see Table 1 for patients' characteristics).

Each patient gave his/her informed consent for collection of clinical data, the cryopreservation of bone marrow samples and the performance of DNA-analysis for scientific purposes, in accordance with institutional guidelines.

Bone marrow samples from each patient were collected and cryopreserved at diagnosis and then centrally analyzed for *KIT* gene mutational status at the Department of Biology and Genetics for Medical Sciences, University of Milan, Italy.

For each patient, data regarding haematologic parameters, bone marrow morphology, immunophenotype, cytogenetic, molecular analysis, diagnosis of EML, treatment schedule and outcome were recorded. The study started in January 2001. Until January 2010, patients' data were periodically updated from the participating centers, centrally verified for consistency and completeness and subsequently submitted for statistical analysis. The study design adhered to the Declaration of Helsinki and approval for this study was obtained from the Niguarda Hospital Review Board.

Patients were enrolled in intensive chemotherapy protocols, as previously described [30]. In brief, they received a standard induction therapy with an anthracycline-containing regimen, most commonly the "7+3" regimen with cytarabine in seven-day continuous intravenous infusion and three doses of anthracycline (idarubicin 12 mg/m^2/day or daunorubicin 60 mg/m^2/day) or the "ICE" schedule, including etoposide 100 mg/m^2/day on days 1-5.

The post-remission chemotherapy consisted of 3 consolidation courses. In patients treated with the "7+3" regimen, the first cycle was with high-dose cytarabine (3000 mg/m^2 every 12 hours for 3 consecutive days, with patients older than 50 years receiving a reduced dose at 2000 mg/m^2) and idarubicin 10 mg/m^2/day on days 1 and 3, while patients treated with ICE schedule received a NOVIA course (mitoxantrone 12 mg/m^2/day on days 1-4 and cytarabine 500 mg/m^2 every 12 hours for 6 doses). The second and third consolidation courses consisted of high-dose cytarabine.

The conditioning regimen for both autologous stem cell transplantation (ASCT) and allogeneic stem cell transplantation (allo-SCT) was with cyclophosphamide 60 mg/kg/day for 2 days and total-body irradiation in 6 fractions of 200 cGy (1200 cGy) or busulfan 16 mg/kg over 4 days and cyclophosphamide 50 mg/kg over 4 days.

2.2. Definitions and criteria for treatment response

Complete remission (CR) was defined as less than 5% of bone marrow blasts, regression of extramedullary disease, transfusion independency with peripheral neutrophil count greater than $1.0x10^9$/L and platelet count greater than $100x10^9$/L and disappearance of the cytogenetic and molecular markers [34-35]. Recurrent disease is defined as the reappearance of more than or equal to 5% blasts in the bone marrow or in the peripheral blood or as the appearance of a new extramedullary site of disease in patients with a previously documented CR.

Extramedullary disease was defined as any leukemic collection outside the bone marrow and its presence was documented either by histological, cytological or radiological criteria.

Overall survival (OS) was calculated from the date of diagnosis until death, where all living patients were censored at the time of last contact. The duration of CR was calculated from the date of the first CR until the date of the first relapse. Relapse incidence (RI) was calculated from the date of the first CR until the date of the first relapse, where patients were censored at the time of last contact or death not due to recurrent disease.

2.3. Screening of mutations in the coding region of KIT gene

Bone marrow samples were submitted for a centralized analysis for *KIT* gene mutations in exon 2, 8, 10, 11 and 17. Mutations of exon 17 were detected using sequencing and other sensitive assays such as enzymatic digestion with *Hin*fI for Asp816Val and with Tsp509I for Asn822Lys and ARMS (amplification refractory mutation system) polymerase chain reaction (PCR) for Asp816Tyr and Asp816His [22,36,37]. Direct sequencing of DNA and cDNA products was performed using Thermo Sequence Dye Terminator sequencing reaction and ABI Prism 3100 sequencing analyzer (Applied Biosystems,Warrington, United Kingdom).

2.4. Statistical analyses

All collected variables were submitted to usual descriptive methods. In particular, for continuous variables the distribution was firstly evaluated by the Shapiro-Wilk test, so that normally distributed variables were summarized with mean and standard deviation, while non-normal variables were summarized with median and range.

The Pearson's chi-square test with Yates' correction for continuity and the Fisher's exact test (if applicable) were used to check the association between categorical data, after cross-tabulation. Comparisons of normally distributed continuous variables were carried out by Student's t-test or by Welch test (in the case of non-homogeneous variances between groups, previously verified by Levene's test). The Mann-Whitney U test was used for comparison of continuous non-normally distributed variables.

The survival analysis was carried out using the Kaplan-Meier product limit method, followed by the log-rank test, to evaluate the possible differences in survival between groups.

Cox univariate and multivariate regression models were also used to analyse the effects of continuous variables on survivorship. The optimal multivariate model was chosen using a backward stepwise elimination after inserting all variables showing $P<0.20$ at univariate analysis.

The receiver operating characteristics curve (ROC) was traced to analyse the role of patients' age on survivorship and to search for an optimal cut-off value for age itself. For all possible cut-off points, the total accuracy was considered together with sensitivity, specificity, positive predictive value and negative predictive value and the cut-off choice was made according to Youden.

Statistical analysis was done using Stata/SE 11.1 (The StataCorp, College Station, TX). Statistical significance was assumed for all tests with $P<0.05$. The Bonferroni method was used to adjust significance in case of multiple comparisons.

3. Results

3.1. *Overall results of treatments*

Fifty-eight patients, aged between 15 and 60 years (median age: 42 years; male/female: 40/18), underwent treatment as described and were assessed for response. CR was obtained from 56 out of 58 (96.5%) patients. Primary refractory disease and one infectious complication during post-chemotherapy aplasia accounted for the two *KIT*-negative patients (aged 57 and 60 years, respectively) who did not achieve CR. A toxic death was subsequently recorded during the consolidation therapies. Twelve patients underwent ASCT instead of the third consolidation course and 2 *KIT*-negative patients received an allo-SCT in the first complete remission (CR1) from a sibling donor.

The median follow-up time for patients was 50 months based on the reverse Kaplan-Meier method. The estimated 5-year OS and RI resulted 69.2% and 48.4%, respectively, with 32 patients alive in CR1 and 11 patients alive in second or subsequent CR (Fig. 1A-2A and Table 2).

3.2. Relapse incidence and survival after relapse

Twenty-four out of 56 patients who achieved CR experienced relapse, including 4 patients who received an ASCT in CR1. The RI plot grew up rapidly to 43.6% within 17.7 months and reached 48.4% at 38.2 months (Fig. 2A). Twenty-three out of 24 patients underwent salvage chemotherapy, while 1 patient was lost at follow-up. The median survival time after relapse was 14.7 months (range: 1.1-92.4), with 17 (74%) patients achieving a second complete remission (CR2) and 6 (26%) dying for resistant relapse. Eleven patients underwent a stem cell transplantation (1 ASCT, 10 allo-SCT) in CR2. Of them, 8 allo-transplanted patients were alive and disease-free with a median CR2 duration of 30.8 months (range: 1.0-91.4), and 3 patients died for transplant-related mortality. The remaining 6 patients who entered the CR2 received intensive consolidation chemotherapy courses: 4 patients presented a second relapse and 3 of them subsequently died from disease progression (Table 2). Overall, 11 out of 23 (47.8%) relapsed patients are still alive and disease-free, with a median CR2 duration of 19.0 months (range: 1.0-91.4).

3.3. Incidence of KIT mutations and correlation between KIT status and clinical characteristics

Mutational screening reported *KIT* gene mutations in 15 of 58 patients (25.9%): 12 (20.6 %) patients showed a D816 missense mutation (TKD^{816}), 2 (3.4%) patients presented an Exon 8 in-frame deletion plus insertion mutations, 1 (1.7%) patient had an Exon 10 (V530I) transmembrane mutation (Table 1). Patients with *KIT* gene mutations were classified as "*KIT*-positive" (KIT^+), while the remaining 43 patients who showed no mutations were classified as "*KIT*-negative" (KIT^-). Statistical analysis showed no significant difference in term of age (*P*=0.368), sex ratio (*P=0.*756) and WBC count at diagnosis (*P*=0.765) between KIT^+ and KIT^- patients.

Seven patients out of the 58 cases included in this study (12.0%) had EML at presentation. In all cases the EML manifested in form of myeloid sarcoma involving a variety of sites (spinal masses, gastrointestinal tract, lungs) except for skin. The association between the *KIT* mutational status and EML turned out to be not significant (*P*=0.360).

3.4. Treatment outcome by KIT mutational status

Complete remission was achieved in 100.0% (15/15) of KIT^+ patients after induction therapy. Recurrent disease was observed in 9 (60.0%) and 15 (34.9%) patients of KIT^+ and KIT^- group, respectively. No difference was seen in term of RI between KIT^+ and KIT^- patients (*P*=0.166), with an estimated 5-year RI of 65.5% and 41.8%, respectively (Fig. 2B). Similarly, OS was not affected by *KIT* mutational status (*P*=0.569), with an estimated 5-year OS of 62.3% and 72.1% for KIT^+ and KIT^- patients, respectively (Fig. 1B). Resistant relapses (4 patients) and one transplant-related death accounted for the 5 KIT^+ deceased patients (Table 3).

3.5. Prognostic factors for overall survival and relapse incidence

Cox univariate and multivariate regression models were performed to evaluate the role of different clinical variables as predictors for relapse or survival. The following potential prognostic parameters were evaluated: age, sex, WBC count at diagnosis, EML, *KIT* status and presence at standard cytogenetic of trisomy of chromosome 22. For continuous variables (age and WBC), a receiver operating characteristic (ROC) curve analysis was performed towards survival in search of possible cut-off values. Age distribution showed an optimal cut-point at 43 years (AUC 0.827, sensitivity 93.3%, specificity 68.3; *P*=0.0001), while no possible cut-off points for WBC were identified.

In univariate analyses, only age, both as continuous or dichotomous variable with cut-off point set at 43 years, showed prognostic significance for OS (*P*<0.00005) (Fig. 1C), while no statistical significance was found for all the other variables. When combined in the multivariate analyses, only age both as continuous or dichotomous variable was a significant part of the Cox model and proved to be an independent risk factor for OS (*P*<0.001). Any increase of one year in age led to a 15% increase (*P*<0.0005) of the hazard of death, while being 43 years old or more implied a hazard ratio of 47.41 (95% CI, 4.87 to 461.39; *P*=0.004), adjusting by WBC, EML and *KIT* mutational status (Table 4).

In the multivariate Cox model with backward elimination of factors, WBC emerged as an independent risk factor for RI (*P*=0.017) and any 1.0x10^9/L increment of WBC meant a 1.1% increase of the hazard of relapse (95% CI, 1.002 to 1.020; *P*=0.017), adjusting by age and *KIT* mutational status (Table 4). *KIT* mutations showed a trend for RI but did not reach a significative value (*P*=0.069).

4. Discussion

In the present study, we have evaluated the impact of clinical and genetic features on the prognosis of *de novo* AML with inv(16)/t(16;16) in 58 patients with age less than or equal to 60 years, treated according to standard chemotherapy protocols. Overall, we observed an high CR rate (96.5%), a RI of 48.4% at 38.2 months after the first CR and an estimated 5-year OS of 69.2%, according to outcome data reported in the recent literature. In this relative large cohort of homogeneously treated patients, we found that only WBC at presentation and age emerged as an independent risk factor for relapse (*P*=0.017) and overall survival (*P*<0.001), respectively.

A high peripheral WBC count together with a raised serum LDH, the presence of hepatosplenomegaly and EML, may reflect an increased tumour burden in AML even in the setting of "good risk" acute leukemias, such as acute promyelocytic leukemia or CBF-AML [19,38-40]. In AML with inv(16), Delaunay *et al.* reported that bad prognosis factors for CR achievement were a high WBC count, with an optimal cut-off point at 120x10^9/L, and lower platelet count [20]. Martin *et al*., in a small study, found that presenting WBC count had a significant negative influence on disease-free survival [19]. Our data are substantially in line with reported data, therefore we found an increase of 1.1% hazard of relapse for each 1.0x10^9/L increment of WBC count. However, we were not able to identify any possible WBC cut-off value by means of the ROC analysis.

Activating *KIT* mutations are frequently found in CBF leukemia [41]. We recorded here an incidence of 25.9% of *KIT* mutations, with most patients showing a D816 missense mutations (Table 1). From this aspect, it is of interest that expression levels of both *KIT* mRNA and proteins is much higher in CBF-AML, with either wild type or mutant *KIT*, than in leukemia cells negative for core binding factor rearrangements. Moreover, we recently reported that CBF genetic abnormalities, in addition to directly targeting and down-regulating the expression of hematopoietic protein-coding genes containing AML1 consensus sequences, can target microRNA genes (Mir222/221) involved in the regulation of the *KIT* receptor leading to *KIT* overexpression in CBF-AML [42]. Furthermore, it has been postulated that mutations of the *KIT* gene may drive the WBC proliferation in CBF leukemia. Recently, Luck *et al.*, showed that *KIT* mutations confer a distinct gene expression signature in CBF-AML and that one of the most significantly differentially expressed gene is LRP6 that is essential for non-canonical WNT5A signaling and thus for the maintenance of stem and progenitor cells [43,44]. Authors suggested that the different gene profiling may lead to an enhancement of proliferation in the *KIT*-mutated cases, which may be reflected in the higher blast counts of those patients [43]. The clinical observations that affected patients with t(8;21) appear to have an higher WBC count and WBC-index at presentation and a higher frequency of EML might support this hypotheses [30,39,45].

However, despite these reports on AML with t(8;21), we did not find any difference in WBC count (*P*=0.765) and incidence of EML (*P*=0.360) between the 15 KIT^+ and the 43 KIT^- cases harbouring the inv(16)/t(16;16) recruited in this study. Similarly, regarding the impact on outcome, this study showed that *KIT* mutations did

not reach a significative value as independent prognostic factor for relapse and survival neither in the multivariate nor in the Kaplan-Meier analysis, in contrast to those reported in adult patients with t(8;21) (Fig. 1B-2B and Tables 3-4) [24,26-28,30-32].

Accumulating evidence suggests that a high degree of similarity is identified between the two major subtypes of CBF leukemias. However, important differences on clinical and biological ground are reported [1,2]. A recent study using Drosophila as a model showed that AML1-ETO-expressing precursor cells express high levels of reactive oxygen species (ROS), and that ROS plays a central role in the proliferation of these precursors [46]. As for CBFβ-MYH11 leukemia, gene expression profiling of AML-M4 subtype suggested a highly activated NF-kB pathway in inv(16) patients [47]. Given that these pathways, particularly Notch, Wnt, and Cox/PGE2 signaling, are essential for stem cell self renewal, they could contribute to a different transforming activity of AML1-ETO and CBFβ -MYH11 in CBF-AML.

Although our data suggest that a high WBC count is an unfavourable prognostic factor, since it increases the risk of relapse in multivariate analysis, it shows no significant effect on overall survival. In fact, after salvage and subsequent therapy including allo-SCT, we found that 11 out of 23 relapsed patients who underwent salvage chemotherapy are still alive and disease-free, with a median second CR duration of 19 months.

In this study, only age as continuous or dichotomic value, with a best calculated cut-off point at 43 years, emerges as a prognostic factor affecting survival in both univariate or multivariate analysis. It is to be noted that, among the 30 patients aged 42 years or younger, we recorded only one death (transplant related), leading to a Kaplan-Meier plot of 95.5% for OS (P<0.00005) (Table 2 and Fig. 1C). By contrary, focusing on 28 patients aged 43 years or older, we recorded 14 deaths (2 early deaths, 1 death in aplasia, 2 deaths for transplant-related complications and 9 for first or second resistant relapse). Overall, 50% of patients aged 43 years or older are disease-free at 27.1 months (Table 2 and Fig. 2C).

Our data confirm that the strategy to perform an allogeneic SCT in CR>1 lead to encouraging results. In fact, of 10 patients allo-transplanted while in second CR, eight (80%) are alive and disease-free, with a median follow-up of 30.8 months. As in our study, Kuwatsuka et al., of 66 patients with inv(16) undergoing allo-SCT, reported an OS of 86% at 3 years in second or third CR and identified only age to be a significant prognostic factor. The Japanese study concluded that allo-SCT is not necessarily recommended for inv(16) in first CR and that inv(16) patients who received an allo-SCT not in CR did significantly better than those with t(8;21) [2]. Furthermore, a French survey reported that age, with a best cut-off at 35 years, was the only factor for shorter disease-free survival in AML with inv(16) [20].

It has been repeatedly demonstrated that prognosis worsens with increasing age in AML [48,49]. This may reflect concurrent co-morbidities in addition to different disease biology such as multidrug resistance protein (MDR-1) positivity or stem cell phenotype adversely affecting both attainment of remission and refractory relapse risk [49,50].

Paschka *et al.* reported that in inv(16) patients the cumulative incidence of relapse (CIR) was higher for *KIT*-positive patients, especially if presenting exon 17 mutation, compared with *KIT*-negative patients (5-year CIR 80% *vs* 29%; P=0.002). Furthermore, the authors reported that *KIT* mutations predicted worse survival when adjusted for sex [24]. Anyway, it has to be noted that in the CALGB study the *KIT*-mutated patients were significantly older (median age: 38 *vs* 49 years; P<0.001) and were more frequently male (P<0.05) compared with non mutated patients. Moreover, in the reviewed literature, all the studies focused on the prognostic significance of *KIT* mutations in the CBFβ-MYH11 adult patients have been unable to replicate the CALGB

conclusions on survival and, to our knowledge, all studies but one [26] do not show any influence of *KIT* mutations on relapse [27,30-32].

All the results reported in these different studies are based on a relatively small population, principally due to the fact that AML is a rare disease and that the CBFβ subtype accounts for about 5-8% of adults with *de novo* AML. In a nine-years period (January 2001-January 2010) we considered 58 patients aged less than or equal to 60 years belonging from 8 Italian centers. At present, this is one of the studies with the largest number of adult CBFβ AML patients, second only to the one of Paschka and colleagues (counting 61 patients). Incrementing the number of patients surely would be of interest, but when it results in an excessive accrual time statistical analysis it is more likely to be biased.

In conclusion, while the prognostic significance of *KIT* mutations remains unclear with several studies yielding contrasting results [24,26,27,30-32], our data showed that only "old" prognostic factors, such as age and the WBC count at diagnosis, are important predictors of outcome in AML adult patients with inv(16)/t(16;16).

Conflict of interest statement

The authors reported no potential conflicts of interest.

Acknowledgements

Contributions. RC was the principal investigator and takes primary responsibility for the paper. MT, GB, GN, FR, CC, FF, GP, EP, GR, GM and EM recruited the patients. AB and FL performed the laboratory work for this study. MT and GB verified patients' data for consistency and completeness. MT and MN participated in the statistical analysis. RC, MT and AB wrote the paper.

References

[1] Marcucci G, Mrozek K, Ruppert AS, Maharry K, Kolitz JE, Moore JO, et al. Prognostic factors and outcome of core binding factor acute myeloid leukemia patients with t(8;21) differ from those of patients with inv(16): a Cancer and Leukemia roup B study. J Clin Oncol. 2005;23:5705-17.

[2] Kuwatsuka Y, Miyamura K, Suzuki R, Kasai M, Maruta A, Ogawa H, et al. Hematopoietic stem cell transplantation for core binding factor acute myeloid leukemia: t(8;21) and inv(16) represent different clinical outcomes. Blood. 2009;113:2096-103.

[3] Wong KF, Kwong YL. Trisomy 22 in acute myeloid leukemia: a marker for myeloid leukemia with monocytic features and cytogenetically cryptic inversion 16. Cancer Genet Cytogenet. 1999;109:131-3.

[4] Le Beau MM, Larson RA, Bitter MA, Vardiman JW, Golomb HM, Rowley JD. Association of an inversion of chromosome 16 with abnormal marrow eosinophils in acute myelomonocytic leukemia: A unique cytogenetic clinicopathological association. N Engl J Med. 1983;309:630-6.

[5] Byrd JC, Mrozek K, Dodge RK, Carrol AJ, Edwards CG, Arthur DC, et al. Pretreatment cytogenetic abnormalities are predictive of induction success, cumulative incidence of relapse, and overall survival in adult patients with de novo acute myeloid leukemia: results from Cancer and Leukemia Group B (CALGB 8461). Blood. 2002;100:4325-36.

[6] Mrozek K, Heinonen K, de la Chapelle A, Bloomfield CD. Clinical significance of cytogenetics in acute myeloid leukemia. Semin Oncol. 1997;24:17-31.

[7] Marlton P, Keating M, Kantarjian H, Pierce S, O'Brien S, Freireich EJ, et al. Cytogenetic and clinical correlates in AML patients with abnormalities of chromosome 16. Leukemia. 1995;9:965-71.

[8] Bloomfield CD, de la Chapelle A. Chromosome abnormalities in acute nonlymphocytic leukemia: Clinical and biologic significance. Semin Oncol. 1987.14:372-83.

[9] Billstrom R, Ahlgren T, Bekassy AN, Malm C, Olofsson T, Hoglund M, et al. Acute myeloid leukemia with inv(16)(p13q22): involvement of cervical lymph nodes and tonsils is common and may be a negative prognostic sign. Am J Hematol. 2002;71:15-9.

[10] Appelbaum FR, Kopecky KJ, Tallman MS, Slovak ML, Gundacker HM, Kim HT, et al. The clinical spectrum of adult acute myeloid leukaemia associated with core binding factor translocations. Br J Haematol. 2006;135:165-73.

[11] Grimwade D, Walker H, Oliver F, Wheatley K, Harrison C, Harrison G, et al. The importance of diagnostic cytogenetics on outcome in AML: analysis of 1,612 patients entered into the MRC AML 10 trial. Blood. 1998;92:2322-33.

[12] Larson RA, Williams SF, Le Beau MM, Bitter MA, Vardiman JW, Rowley JD. Acute myelomonocytic leukemia with abnormal eosinophils and inv(16) or t(16;16) has a favorable prognosis. Blood. 1986;68:1242-9.

[13] Bloomfield CD, Shuma C, Regal L, Philip PP, Hossfeld DK, Hagemeijer AM, et al. Longterm survival of patients with acute myeloid leukemia: a third follow-up of the Fourth International Workshop on Chromosomes in Leukemia. Cancer. 1997;80:2191-8.

[14] Bloomfield CD, Lawrence D, Byrd JC, Carroll A, Pettenati MJ, Tantravahi R, et al. Frequency of prolonged remission duration after high-dose cytarabine intensification in acute myeloid leukemia varies by cytogenetic subtype. Cancer Res. 1998;58:4173-9.

[15] Marcucci G, Caligiuri MA, Bloomfield CD. Molecular and clinical advances in core binding factor primary acute myeloid leukemia: a paradigm for translational research in malignant hematology. Cancer Invest. 2000;18:768-80.

[16] Byrd JC, Ruppert AS, Mrozek K, Carroll AJ, Edwards CG, Arthur DC, et al. Repetitive cycles of high-dose cytarabine benefit patients with acute myeloid leukemia and inv(16)(p13q22) or t(16;16)(p13;q22): Results from CALGB 8461. J Clin Oncol. 2004;22:1087-94.

[17] Mrozek K, Bloomfield CD. Chromosome aberrations, gene mutations and expression changes, and prognosis in adult acute myeloid leukemia. Hematology Am Soc Hematol Educ Program. 2006,169-77.

[18] Schlenk RF, Benner A, Hartmann F, del Valle F, Weber C, Pralle H, et al. Risk-adapted postremission therapy in acute myeloid leukemia: Results of the German multicenter AML HD93 treatment trial. Leukemia. 2003;17:1521-8.

[19] Martin G, Barragan E, Bolufer P, Chillon C, Garcia-Sanz R, Gomez T, et al. Relevance of presenting white blood cell count and kinetics of molecular remission in the prognosis of acute myeloid leukemia with CBFbeta/MYH11 rearrangement. Haematologica. 2000;85:699-703.

[20] Delaunay J, Vey N, Leblanc T, Fenaux P, Rigal-Huguet F, Witz F, et al. Prognosis of inv(16)/t(16;16) acute myeloid leukemia (AML): A survey of 110 cases from the French AML Intergroup. Blood. 2003;102:462-9.

[21] Schlenk RF, Benner A, Krauter J, Büchner T, Sauerland C, Ehninger G, et al. Individual patient data-based meta-analysis of patients aged 16 to 60 years with core binding factor acute myeloid leukemia: a survey of the German Acute Myeloid Leukemia Intergroup. J Clin Oncol. 2004;22:3741-50.

[22] Beghini A, Peterlongo P, Ripamonti CB, Larizza L, Cairoli R, Morra E et al. C-kit mutations in core binding factor leukemias. Blood. 2000;95:726-7.

[23] Longley BJ, Reguera MJ, Ma Y. Classes of C-kit activating mutations; proposed mechanisms of action and implication for disease classification and therapy. Leuk Res. 2001;25:571-6.

[24] Paschka P, Marcucci G, Ruppert AS, Mrozek K, Chen H, Kittles RA, et al. Adverse prognostic significance of KIT mutations in adult acute myeloid leukemia with inv(16) and t(8;21): A Cancer and Leukemia Group B study. J Clin Oncol. 2006;24:3904-11.

[25] The NCCN Clinical Practice Guidelines in Oncology. Acute Myeloid Leukemia (Version 2.2011), 2011 National Comprehensive Cancer Network, Inc. http:www.nccn.org.

[26] Care RS, Valk PJ, Goodeve AC, Abu-Duhier FM, Geertsma-Kleinekoort WM, Wilson GA, et al. Incidence and prognosis of c-KIT and FLT3 mutations in core binding factor (CBF) acute myeloid leukaemias. Br J Haematol, 2003;121:775-7.

[27] Boissel N, Leroy H, Brethon B, Philippe N, de Botton S, Auvrignon A, et al. Incidence and prognostic impact of c-KIT, FLT3, and RAS gene mutations in core binding factor acute myeloid leukemia (CBF-AML). Leukemia. 2006;20:965-70.

[28] Schnittger S, Kohl TM, Haferlach T, Kern W, Hiddemann W, Spiekermann K, et al. KIT-D816 mutations in AML1-ETO-positive AML are associated with impaired event-free and overall survival. Blood. 2006;107:1791-9.

[29] Fuster O, Barragan E, Bolufer P, Cervera J, Larrayoz MJ, Jimenez-Velasco A, et al. Rapid detection of KIT mutations in core-binding factor acute myeloid leukemia using high-resolution melting analysis. J Mol Diagn. 2009;11:458-63.

[30] Cairoli R, Beghini A, Grillo G, Nadali G, Elice F, Ripamonti CB, et al. Prognostic impact of c-KIT mutations in core binding factor leukemia: an Italian retrospective study. Blood. 2006;107:1791-9.

[31] Mrozek K, Marcucci G, Paschka P, Bloomfield CD. Advances in molecular genetics and treatment of core-binding factor acute myeloid leukemia. Curr Opin Oncol. 2008;20:711-8.

[32] Patel JP, Gonen M, Figueroa ME, Ferandez H, Sun Z, Racevskis J, et al. Prognostic relevance of integrated genetic profiling in acute myeloid leukemia. N Engl J Med. 2012;366:1079-89.

[33] Shih LY, Liang DC, Huang CF, Chang YT, Lai CL, Lin TH, et al. Cooperating mutations of receptor tyrosine kinases and Ras genes in childhood core-binding factor acute myeloid leukemia and a comparative analysis on paired diagnosis and relapse samples. Leukemia. 2008;22:303–7.

[34] Morra E, Barosi G, Bosi A, Ferrara F, Locatelli F, Marchetti M, et al. Clinical management of primary non-acute promyelocytic leukemia acute myeloid leukemia: practice Guidelines by the Italian Society of Hematology, the Italian Society of Experimental Hematology and the Italian Group for Bone Marrow Transplantation. Haematologica. 2009;94:102-12.

[35] Cheson BD, Bennett JM, Kopecky KJ, Buchner T, Willman CL, Estey EH, et al. Revised recommendations of the International Working Group for Diagnosis, Standardization of Response Criteria, Treatment Outcomes, and Reporting Standards for Therapeutic Trials in Acute Myeloid Leukemia. J Clin Oncol. 2003;21:4642-9.

[36] Beghini A, Ripamonti CB, Cairoli R, Cazzaniga G, Colapietro P, Elice F, et al. KIT activating mutations: incidence in adult and pediatric AML, and identification of an internal tandem duplication. Haematologica. 2004;89:920-5.

[37] Beghini A, Magnani I, Ripamonti CB, Larizza L. Amplification of a novel c-Kit activating mutation Asn(822)-Lys in the Kasumi-1 cell line: a t(8;21)-Kit mutant model for acute myeloid leukemia. Hematol J. 2002;3:157-63.

[38] Dalley CD, Lister TA, Cavenagh JD, Rohatiner AZ. Serum LDH, a prognostic factor in elderly patients with acute myelogenous leukemia. Br J Cancer. 2001;84:147.

[39] Nguyen S, Leblanc T, Fenaux P, Witz F, Blaise D, Pigneux A, et al. A white blood cell index as the main prognostic factor in t(8;21) acute myeloid leukemia: a survey of 161 cases from the French AML intergroup. Blood. 2002;99:3517-23.

[40] Burnett AK, Grimwade D, Solomon E, Wheatley K, Goldstone AH. Presenting white blood cell count and kinetics of molecular remission predict prognosis in acute promyelocitic leukemia treated with all-trans retinoic acid: result of the randomized MRC trial. Blood. 1999;93:4131-43.

[41] Smith ML, Hills RK, Grimwade D. Independent prognostic variable in acute myeloid leukemia. Blood rev. 2011;25:39-51.

[42] Brioschi M, Fischer J, Cairoli R, Rossetti S, Pezzetti L, Nichelatti M, et al. Down-regulation of MicroRNAs 222/221 in Acute Myelogenous Leukemia with Deranged Core-Binding Factor Subunits. Neoplasia. 2010;12:866-76.

[43] Luck SC, Russ AC, Du J, Gaidzik V, Schlenk RF, Pollack JR, et al. KIT mutations confer a distinct gene expression signature in core binding factor leukaemia. Br J Haematol. 2010;148:925-37.

[44] Katoh M, Katoh M. STAT3-induced WNT5A signaling loop in embryonic stem cells, adult normal tissues, chronic persistent inflammation, rheumatoid arthritis and cancer (Review). Int J Mol Med. 2007;19:273-8.

[45] Cairoli R, Grillo G, Beghini A, Tedeschi A, Ripamonti CB, Larizza L, et al. C-Kit point mutations in core binding factor leukemias: correlation with white blood cell count and the white blood cell index. Leukemia. 2003;17:471-2.

[46] Sinenko SA, Hung T, Moroz T, Tran QM, Sidhu S, Cheney MD, et al. Genetic manipulation of AML1-ETO-induced expansion of hematopoietic precursors in a Drosophila model. Blood. 2010;116:4612-20.

[47] Sun X, Zhang W, Ramdas L, Stivers DN, Jones DM, Kantarjian HM, et al. Comparative analysis of genes regulated in acute myelomonocytic leukemia with and without inv(16)(p13q22) using microarray techniques, real-time PCR, immunohistochemistry, and flow cytometry immunophenotyping. Mod Pathol. 2007;20:811-20.

[48] Appelbaum FR, Gundacker H, Head DR, Slovak ML, Willman CL, Godwin JE, et al. Age and acute myeloid leukemia. Blood. 2006;107:3481-5.

[49] Sekeres MA, Stone RM. The challenge of acute myeloid leukemia in older patients. Curr Opin Oncol. 2002;14:24-30.

[50] Sorror ML, Giralt S, Sandmaier BM, De Lima M, Shahjahan M, Maloney DG, et al. Hematopoietic cell transplantation specific comorbidity index as an outcome predictor for patients with acute myeloid leukemia in first complete remission: combined FHCRC and MDACC experiences. Blood. 2007;110:4606-13.

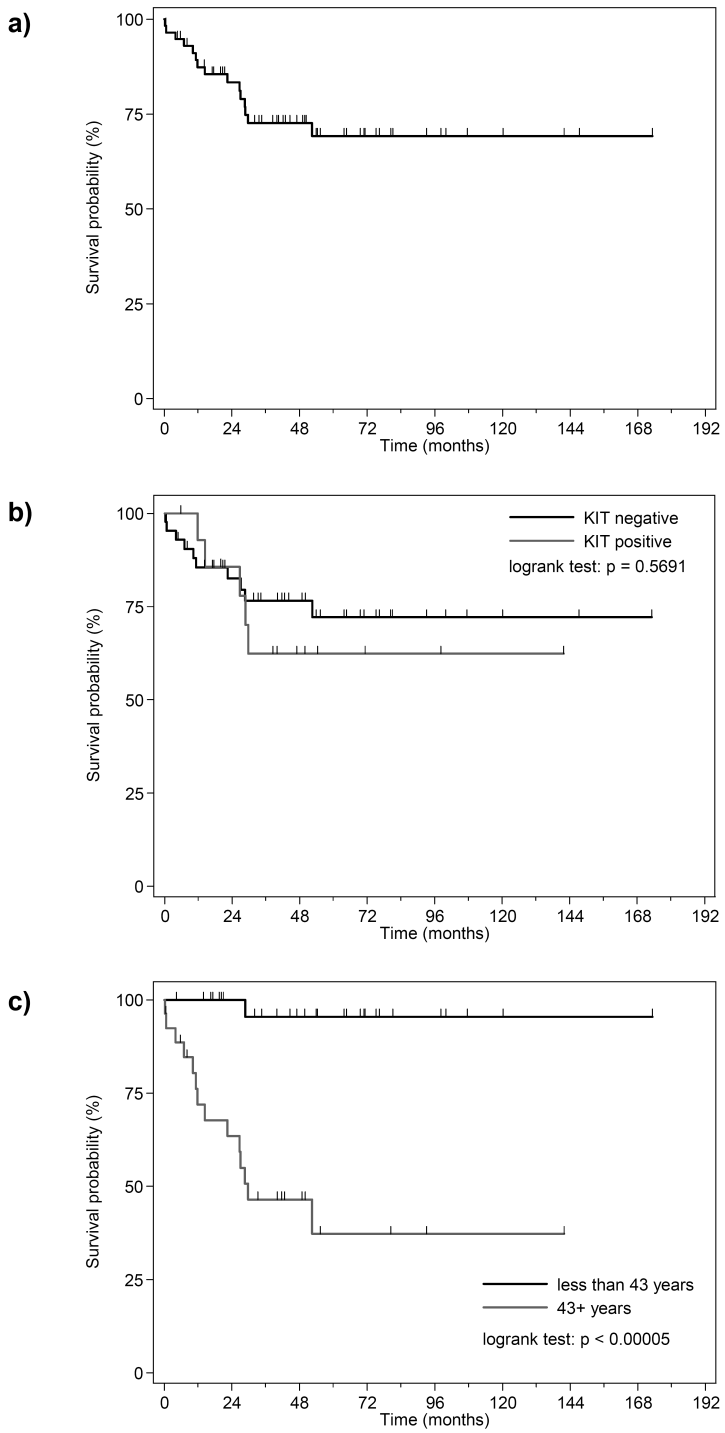

Figure 1. Kaplan-Meier plots showing the probability of survival. (A) Adult patients aged less than or equal to 60 years with inv(16)/t(16;16). The estimated 5-year OS resulted 69.2%. (B) *KIT*-negative (black line) versus *KIT*-positive (gray line) patients. OS was not affected by *KIT* mutational status (*P*=0.5691), with an estimated 5-year OS of 72.1% and 62.3% for *KIT*-negative and *KIT*-positive patients, respectively. (C) Patients aged less than 43 years (black line) or older than or equal to 43 years (gray line). Age showed prognostic significance for OS at a cut-off point set at 43 years (*P*<0.00005), with an estimated 5-year OS of 95.5% and 37.2%, respectively. OS: overall survival.

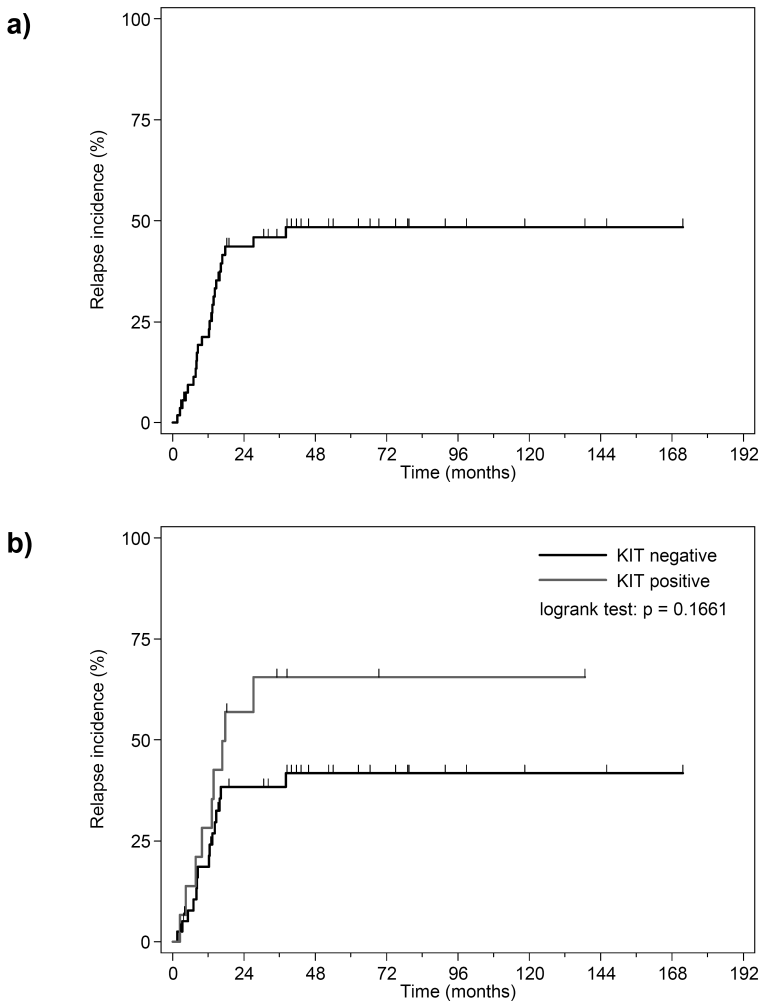

Figure 2. Kaplan-Meier plots showing the relapse incidence. (A) Adult patients aged less than or equal to 60 years with inv(16)/t(16;16). The estimated 5-year RI resulted 48.4%. (B) *KIT*-negative (black line) versus *KIT*-positive (gray line) patients. No difference was seen in term of RI between *KIT*-negative and *KIT*-positive patients (*P*=0.166), with an estimated 5-year RI of 41.8% and 65.5%, respectively. RI: relapse incidence.

Table 1. Clinical characteristics at presentation of patients with inv(16)/t(16;16)

Parameter	**n=58**	
Median age at diagnosis, years (range)	42	(15-60)
Sex (male/female)	40/18	
Median WBC, x 10^9/L (range)	24.7	(1.8-277)
Median marrow blast, % (range)	77.5	(26-95)
Extramedullary disease, no. (%)	7	(12.0)
Cytogenetic features		
Without additional abnormalities (%)	43	(74.1)
No. abnormalities (%)	13*	(22.4)
Including +8	2	
Including +22	6	
Including LOS	1	
Structure abnormalities (%)	3*	(5.2)
Including del(7q)	2	
***KIT* mutational status**		
KIT mutated cases, no. (%)	15	(25.9)
Exon 17	12	
Exon 8	2	
Exon 10	1	

** One patient had both +22 and del(7q). LOS, loss of a sexual chromosome; WBC, white blood cell.*

Table 2. Clinical characteristics and outcome of patients with inv(16)/t(16;16) with recurrent disease

Age, years/ Sex	Cytogenetic at diagnosis	*KIT* status	WBC, x 10^9/L	EML	Status at ASCT	Status at allo-SCT	Outcome	Survival, months
24/M	46,XY,inv(16)(p13q22)	w/t	169,8	Absent	ND	ND	A/1st rel	16,6
26/M	46,XY,inv(16)(p13q22),t(11;12)	V503I	7,6	Absent	ND	ND	A/2nd CR	97,9
29/F	46,XX,inv(16)(p13q22)	D816V	11,1	Gastric mass	ND	2nd CR	A/2nd CR	46,7
32/F	46,XY,inv(16)(p13q22)	w/t	52,3	Absent	ND	2nd CR	A/2nd CR	34,3
36/M	46,XY,inv(16)(p13q22)	w/t	19,0	Absent	ND	2nd CR	A/2nd CR	74,8
36/M	46,XY,inv(16)(p13q22)	w/t	30,4	Absent	ND	2nd CR	A/2nd CR	70,5
36/M	46,XY,inv(16)(p13q22)	w/t	11,3	Absent	ND	ND	A/2nd CR	21,1
36/M	46,XY,inv(16)(p13q22)	D816V	141,0	Absent	1st CR	2nd CR	A/2nd CR	54,0
38/F	46,XX,inv(16)(p13q22)	Exon 8	4,4	Absent	ND	2nd CR	A/2nd CR	49,6
39/M	47,XY,inv(16)(p13q22),+6	w/t	96,2	Absent	ND	2nd CR	A/2nd CR	64,3
42/M	46,XY,inv(16)(p13q22)	w/t	11,7	Mesenteric mass	1st CR	2nd CR	A/2nd CR	107,2
56/F	46,XX,inv(16)(p13q22)	w/t	13,4	Absent	1st CR	ND	A/3rd CR	50,0
43/F	46,XX,inv(16)(p13q22)	w/t	130,0	Absent	ND	2nd CR	D/TRM 2nd CR	27,1
46/M	46,XY,inv(16)(p13q22)	w/t	23,8	Absent	ND	2nd CR	D/TRM 2nd CR	52,6
18/M	46,XY,inv(16)(p13q22)	D816V	12,8	Absent	2nd CR	ND	D/TRM 2nd CR	28,8
60/M	46,XY,inv(16)(p13q22)	w/t	27,7	Absent	ND	ND	D/1st res rel	11,2
47/M	47,XY,inv(16)(p13q22),+22,del(7)	D816H	12,3	Absent	ND	ND	D/1st res rel	29,8
54/F	48,XX, inv(16)(p13q22), +8,+21	w/t	49,8	Absent	ND	ND	D/1st res rel	7,1
52/M	46,XY,inv(16)(p13q22)	w/t	10,9	Ileal mass	ND	ND	D/1st res rel	10,3
55/M	46,XY,inv(16)(p13q22)	D816V	150,0	Absent	ND	ND	D/1st res rel	14,4
58/F	46,XX,inv(16)(p13q22)	D816V	122,0	Absent	ND	ND	D/1st res rel	11,8
50/M	46,XY,inv(16)(p13q22)	w/t	12,0	Absent	1st CR	ND	D/2nd rel	28,6
60/M	48,XY,inv(16) (p13q22),+9,+22	w/t	14,9	Absent	ND	ND	D/2nd res rel	22,4
54/M	46,XY,inv(16)(p13q22)	D816V	110,0	Absent	ND	ND	D/2nd res rel	26,8

A, alive; allo-SCT, allogeneic stem cell transplant; ASCT, autologous stem cell transplant; CR, complete remission; D, dead; EML, extramedullary leukemia; ND, not determined; rel, relapse; res rel, resistant relapse; TRM, transplant related mortality; w/t, wild-type; WBC, white blood cell.

Table 3. Clinical characteristics and outcome of *KIT*-positive patients with inv(16)/t(16;16)

Age, years/ sex	Cytogenetic at diagnosis	*KIT* status	WBC, x 10^9/L	EML	Status at ASCT	Status at allo-SCT	Outcome	Survival, months
18/M	46,XY,inv(16)(p13q22)	D816V	12,8	Absent	2nd CR	ND	D/TRM 2nd CR	28,8
20/M	47,XY,inv(16)(p13q22),+22	D816Y	18,0	Absent	ND	ND	A/1st CR	39,6
26/M	46,XY,inv(16)(p13q22),t(11;12)	V503I	7,6	Absent	ND	ND	A/2nd CR	97,9
29/F	46,XX,inv(16)(p13q22)	D816V	11,1	Gastric mass	ND	2nd CR	A/2nd CR	46,7
36/M	46,XY,inv(16)(p13q22)	D816V	141,0	Absent	1st CR	2nd CR	A/2nd CR	54,0
38/F	46,XX,inv(16)(p13q22)	Exon 8	4,4	Absent	ND	2nd CR	A/2nd CR	49,6
38/M	47,XY,inv(16)(p13q22),+8	D816Y	13,6	Mesenteric mass	ND	ND	A/1st CR	71,0
41/M	46,XY,inv(16)(p13q22)	D816F	13,2	Absent	ND	ND	A/1st CR	19,6
47/M	47,XY,inv(16)(p13q22),+22,del(7)	D816H	12,3	Absent	ND	ND	D/1st res rel	29,8
50/F	46,XY,inv(16)(p13q22)	Exon 8	277,5	Lung	ND	ND	A/1st CR	38,2
51/M	46,XY,inv(16)(p13q22),del(7)	D816F	74,2	Absent	ND	ND	A/1st CR	5,4
53/M	46,XY,inv(16)(p13q22)	D816V	27,3	Absent	ND	ND	A/1st CR	141,5
54/M	46,XY,inv(16)(p13q22)	D816V	110,0	Absent	ND	ND	D/2nd res rel	26,8
55/M	46,XY,inv(16)(p13q22)	D816V	150,0	Absent	ND	ND	D/1st res rel	14,4
58/F	46,XX,inv(16)(p13q22)	D816V	122,0	Absent	ND	ND	D/1st res rel	11,8

Abbreviations are explained in Table 2.

Table 4. Multivariate analysis for overall survival and relapse incidence

Variable	HR	*p*	95% CI	
Overall survival				*(Prob>chi2 = 0.0003)*
AGE	1.148	**0.0003**	1.065	1.237
WBC	1.008	0.252	0.994	1.023
EML	4.605	0.090	0.787	26.930
KIT	1.354	0.651	0.364	5.038
Relapse incidence				*(Prob>chi2 = 0.0271)*
AGE	1.031	0.105	0.994	1.070
WBC	1.011	**0.017**	1.002	1.020
KIT	2.172	0.069	0.940	5.017

CI, confidence interval; EML, extramedullary leukemia; HR, hazard ratio; WBC, white blood cell. Multivariate Cox model for overall survival was adjusted for age, WBC, EML, and KIT. Multivariate Cox model for relapse was adjusted for age, WBC, and KIT.

a)

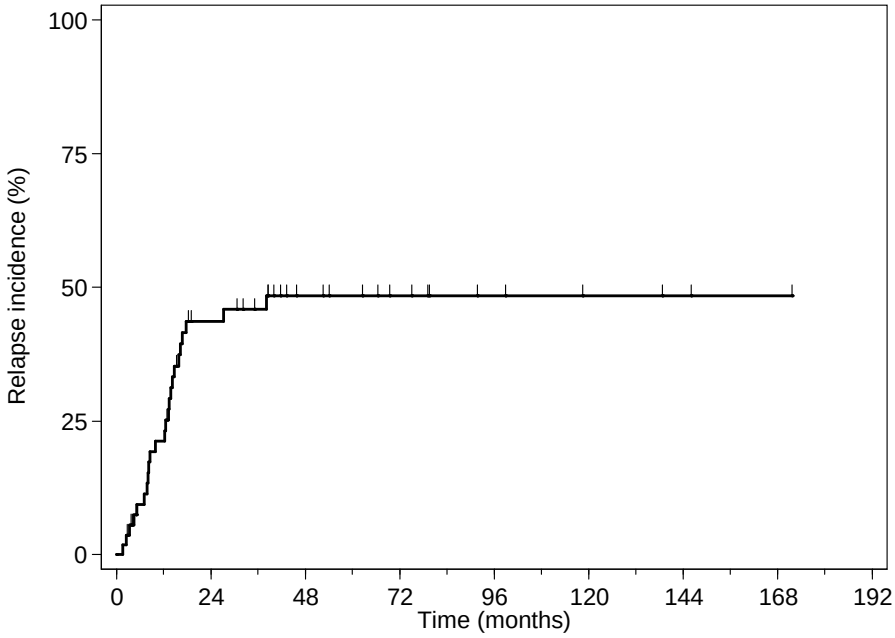
100
75
50
25
0
Relapse incidence (%)
0
24
48
72
96
120
144
168
192
Time (months)

b)

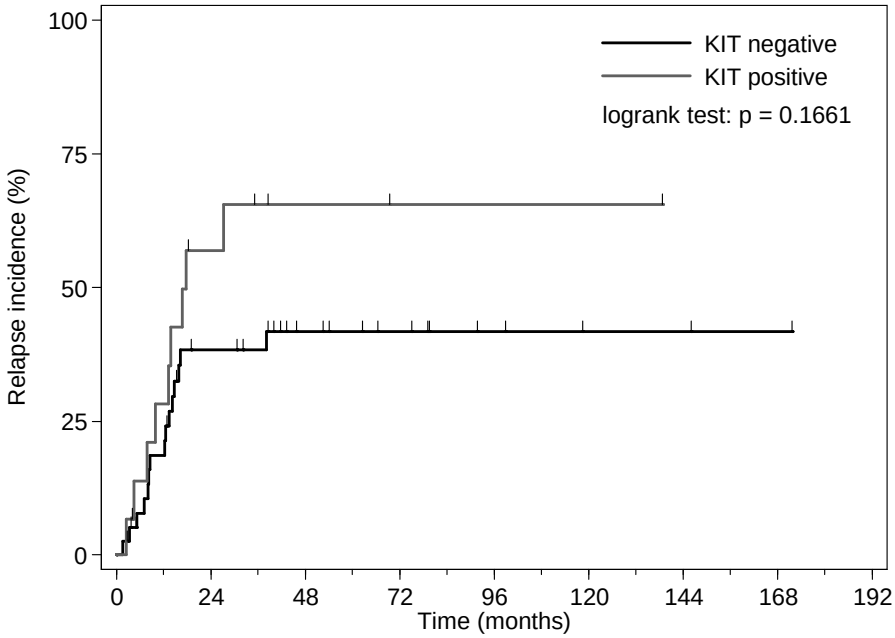
KIT negative
KIT positive
logrank test: p = 0.1661
100
75
50
25
0
Relapse incidence (%)
0
24
48
72
96
120
144
168
192
Time (months)

a)

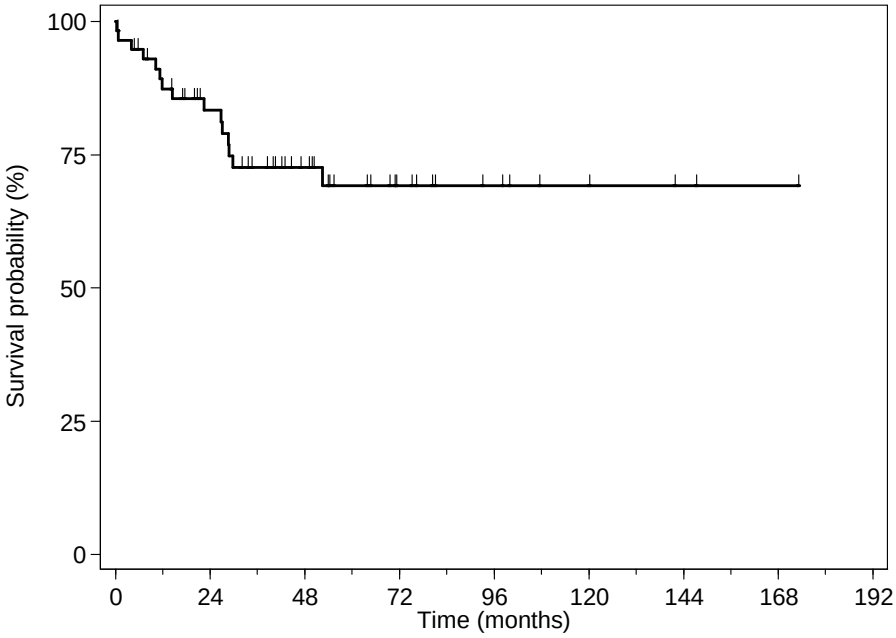
Survival probability (%)
100
75
50
25
0
0
24
48
72
96
120
144
168
192
Time (months)

b)

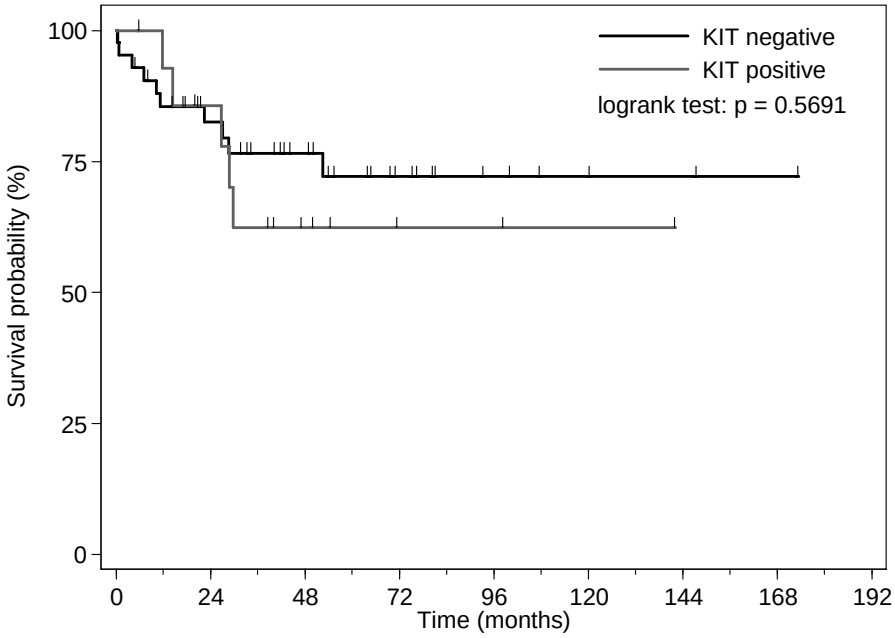
KIT negative
KIT positive
logrank test: p = 0.5691
Survival probability (%)
100
75
50
25
0
0
24
48
72
96
120
144
168
192
Time (months)

c)

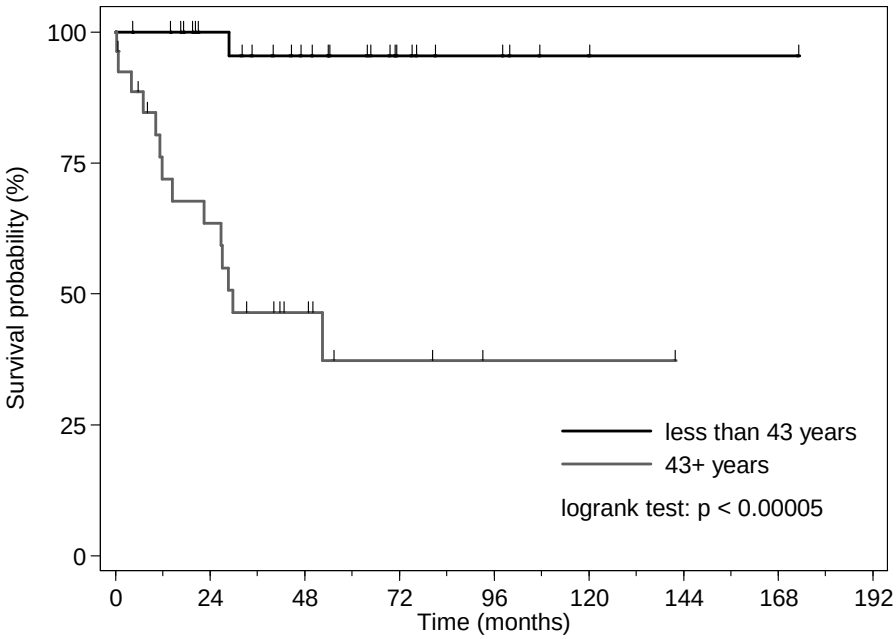
less than 43 years
43+ years
logrank test: p < 0.00005
Survival probability (%)
100
75
50
25
0
0
24
48
72
96
120
144
168
192
Time (months)

Table 1. Clinical characteristics at presentation of patients with inv(16)/t(16;16)

Parameter	**n=58**	
Median age at diagnosis, years (range)	42	(15-60)
Sex (male/female)	40/18	
Median WBC, x 10^9/L (range)	24.7	(1.8-277)
Median marrow blast, % (range)	77.5	(26-95)
Extramedullary disease, no. (%)	7	(12.0)
Cytogenetic features		
Without additional abnormalities (%)	43	(74.1)
No. abnormalities (%)	13*	(22.4)
Including +8	2	
Including +22	6	
Including LOS	1	
Structure abnormalities (%)	3*	(5.2)
Including del(7q)	2	
***KIT* mutational status**		
KIT mutated cases, no. (%)	15	(25.9)
Exon 17	12	
Exon 8	2	
Exon 10	1	

** One patient had both +22 and del(7q). LOS, loss of a sexual chromosome; WBC, white blood cell.*

Table 2. Clinical characteristics and outcome of patients with inv(16)/t(16;16) with recurrent disease

Age, years/ Sex	Cytogenetic at diagnosis	*KIT* status	WBC, x 10^9/L	EML	Status at ASCT	Status at allo-SCT	Outcome	Survival, months
24/M	46,XY,inv(16)(p13q22)	w/t	169,8	Absent	ND	ND	A/1st rel	16,6
26/M	46,XY,inv(16)(p13q22),t(11;12)	V503I	7,6	Absent	ND	ND	A/2nd CR	97,9
29/F	46,XX,inv(16)(p13q22)	D816V	11,1	Gastric mass	ND	2nd CR	A/2nd CR	46,7
32/F	46,XY,inv(16)(p13q22)	w/t	52,3	Absent	ND	2nd CR	A/2nd CR	34,3
36/M	46,XY,inv(16)(p13q22)	w/t	19,0	Absent	ND	2nd CR	A/2nd CR	74,8
36/M	46,XY,inv(16)(p13q22)	w/t	30,4	Absent	ND	2nd CR	A/2nd CR	70,5
36/M	46,XY,inv(16)(p13q22)	w/t	11,3	Absent	ND	ND	A/2nd CR	21,1
36/M	46,XY,inv(16)(p13q22)	D816V	141,0	Absent	1st CR	2nd CR	A/2nd CR	54,0
38/F	46,XX,inv(16)(p13q22)	Exon 8	4,4	Absent	ND	2nd CR	A/2nd CR	49,6
39/M	47,XY,inv(16)(p13q22),+6	w/t	96,2	Absent	ND	2nd CR	A/2nd CR	64,3
42/M	46,XY,inv(16)(p13q22)	w/t	11,7	Mesenteric mass	1st CR	2nd CR	A/2nd CR	107,2
56/F	46,XX,inv(16)(p13q22)	w/t	13,4	Absent	1st CR	ND	A/3rd CR	50,0
43/F	46,XX,inv(16)(p13q22)	w/t	130,0	Absent	ND	2nd CR	D/TRM 2nd CR	27,1
46/M	46,XY,inv(16)(p13q22)	w/t	23,8	Absent	ND	2nd CR	D/TRM 2nd CR	52,6
18/M	46,XY,inv(16)(p13q22)	D816V	12,8	Absent	2nd CR	ND	D/TRM 2nd CR	28,8
60/M	46,XY,inv(16)(p13q22)	w/t	27,7	Absent	ND	ND	D/1st res rel	11,2
47/M	47,XY,inv(16)(p13q22),+22,del(7)	D816H	12,3	Absent	ND	ND	D/1st res rel	29,8
54/F	48,XX, inv(16)(p13q22), +8,+21	w/t	49,8	Absent	ND	ND	D/1st res rel	7,1
52/M	46,XY,inv(16)(p13q22)	w/t	10,9	Ileal mass	ND	ND	D/1st res rel	10,3
55/M	46,XY,inv(16)(p13q22)	D816V	150,0	Absent	ND	ND	D/1st res rel	14,4
58/F	46,XX,inv(16)(p13q22)	D816V	122,0	Absent	ND	ND	D/1st res rel	11,8
50/M	46,XY,inv(16)(p13q22)	w/t	12,0	Absent	1st CR	ND	D/2nd rel	28,6
60/M	48,XY,inv(16) (p13q22),+9,+22	w/t	14,9	Absent	ND	ND	D/2nd res rel	22,4
54/M	46,XY,inv(16)(p13q22)	D816V	110,0	Absent	ND	ND	D/2nd res rel	26,8

A, alive; allo-SCT, allogeneic stem cell transplant; ASCT, autologous stem cell transplant; CR, complete remission; D, dead; EML, extramedullary leukemia; ND, not determined; rel, relapse; res rel, resistant relapse; TRM, transplant related mortality; w/t, wild-type; WBC, white blood cell.

Table 3. Clinical characteristics and outcome of *KIT*-positive patients with inv(16)/t(16;16)

Age, years/ sex	Cytogenetic at diagnosis	*KIT* status	WBC, x 10^9/L	EML	Status at ASCT	Status at allo-SCT	Outcome	Survival, months
18/M	46,XY,inv(16)(p13q22)	D816V	12,8	Absent	2nd CR	ND	D/TRM 2nd CR	28,8
20/M	47,XY,inv(16)(p13q22),+22	D816Y	18,0	Absent	ND	ND	A/1st CR	39,6
26/M	46,XY,inv(16)(p13q22),t(11;12)	V503I	7,6	Absent	ND	ND	A/2nd CR	97,9
29/F	46,XX,inv(16)(p13q22)	D816V	11,1	Gastric mass	ND	2nd CR	A/2nd CR	46,7
36/M	46,XY,inv(16)(p13q22)	D816V	141,0	Absent	1st CR	2nd CR	A/2nd CR	54,0
38/F	46,XX,inv(16)(p13q22)	Exon 8	4,4	Absent	ND	2nd CR	A/2nd CR	49,6
38/M	47,XY,inv(16)(p13q22),+8	D816Y	13,6	Mesenteric mass	ND	ND	A/1st CR	71,0
41/M	46,XY,inv(16)(p13q22)	D816F	13,2	Absent	ND	ND	A/1st CR	19,6
47/M	47,XY,inv(16)(p13q22),+22,del(7)	D816H	12,3	Absent	ND	ND	D/1st res rel	29,8
50/F	46,XY,inv(16)(p13q22)	Exon 8	277,5	Lung	ND	ND	A/1st CR	38,2
51/M	46,XY,inv(16)(p13q22),del(7)	D816F	74,2	Absent	ND	ND	A/1st CR	5,4
53/M	46,XY,inv(16)(p13q22)	D816V	27,3	Absent	ND	ND	A/1st CR	141,5
54/M	46,XY,inv(16)(p13q22)	D816V	110,0	Absent	ND	ND	D/2nd res rel	26,8
55/M	46,XY,inv(16)(p13q22)	D816V	150,0	Absent	ND	ND	D/1st res rel	14,4
58/F	46,XX,inv(16)(p13q22)	D816V	122,0	Absent	ND	ND	D/1st res rel	11,8

Abbreviations are explained in Table 2.

Table 4. Multivariate analysis for overall survival and relapse incidence

Variable	HR	*p*	95% CI	
Overall survival				*(Prob>chi2 = 0.0003)*
AGE	1.148	**0.0003**	1.065	1.237
WBC	1.008	0.252	0.994	1.023
EML	4.605	0.090	0.787	26.930
KIT	1.354	0.651	0.364	5.038
Relapse incidence				*(Prob>chi2 = 0.0271)*
AGE	1.031	0.105	0.994	1.070
WBC	1.011	**0.017**	1.002	1.020
KIT	2.172	0.069	0.940	5.017

CI, confidence interval; EML, extramedullary leukemia; HR, hazard ratio; WBC, white blood cell. Multivariate Cox model for overall survival was adjusted for age, WBC, EML, and KIT. Multivariate Cox model for relapse was adjusted for age, WBC, and KIT.

Figure Legends

Figure 1

Kaplan-Meier plots showing the probability of survival. (A) Adult patients aged less than or equal to 60 years with inv(16)/t(16;16). The estimated 5-year OS resulted 69.2%. (B) *KIT*-negative (black line) versus *KIT*-positive (gray line) patients. OS was not affected by *KIT* mutational status (P=0.5691), with an estimated 5-year OS of 72.1% and 62.3% for *KIT*-negative and *KIT*-positive patients, respectively. (C) Patients aged less than 43 years (black line) or older than or equal to 43 years (gray line). Age showed prognostic significance for OS at a cut-off point set at 43 years (P<0.00005), with an estimated 5-year OS of 95.5% and 37.2%, respectively. OS: overall survival.

Figure 2

Kaplan-Meier plots showing the relapse incidence. (A) Adult patients aged less than or equal to 60 years with inv(16)/t(16;16). The estimated 5-year RI resulted 48.4%. (B) *KIT*-negative (black line) versus *KIT*-positive (gray line) patients. No difference was seen in term of RI between *KIT*-negative and *KIT*-positive patients (P=0.166), with an estimated 5-year RI of 41.8% and 65.5%, respectively. RI: relapse incidence.

Table Legends

Table 1

Clinical characteristics at presentation of patients with inv(16)/t(16;16)

LOS, loss of a sexual chromosome; WBC, white blood cell.

* One patient had both +22 and del(7q).

Table 2

Clinical characteristics and outcome of patients with inv(16)/t(16;16) with recurrent disease

A, alive; allo-SCT, allogeneic stem cell transplant; ASCT, autologous stem cell transplant; CR, complete remission; D, dead; EML, extramedullary leukemia; ND, not determined; rel, relapse; res rel, resistant relapse; TRM, transplant related mortality; w/t, wild-type; WBC, white blood cell.

Table 3

Clinical characteristics and outcome of KIT-positive patients with inv(16)/t(16;16)

Abbreviations are explained in Table 2.

Table 4

Multivariate analysis for overall survival and relapse incidence

CI, confidence interval; EML, extramedullary leukemia; HR, hazard ratio; WBC, white blood cell. Multivariate Cox model for overall survival was adjusted for age, WBC, EML, and KIT. Multivariate Cox model for relapse was adjusted for age, WBC, and KIT.

Contributed by: Lazzaroni F. and Beghini A.

PTPN6 protein tyrosine phosphatase, non-receptor type 6 [*Homo sapiens*]

Identity

- **Other names:** HCP; HCPH; SHP1; SHP-1; HPTP1C; PTP-1C; SHP-1L; SH-PTP1.
- **HGNC (Hugo):** HGNC:9658
- **Ensembl:** ENSG00000111679
- **UniProt KB:** P29350
- **LocusID (NCBI):** 5777
- **Location:** 12p13.31
- **Location base pair:** Chromosome12 (7055740- 7070479).
- **Orientation :** plus strand.

DNA

- **Description:** spans 14740 bp. The PTPN6 gene is divided in **17 exons**. A notable feature of the PTPN6 gene is that it has two promoter regions. Whereas the distal promoter, **P1**, located upstream of the very short exon 1 (also known as exon 1a) is active in epithelial cells, the proximal promoter **P2** that initiates gene transcription from exon 2 (known as exon 1b), is utilized by the hematopoietic cells. The function of P1 promoter has been partially elucidated, while the structure and regulatory mechanism of the P2 promoter remain essentially unknown.

  Recent works, characterized the hematopoietic cell-specific P2 promoter of PTPN6 gene as well as identified the **PU.1** transcription factor as the activator of the P2 promoter.

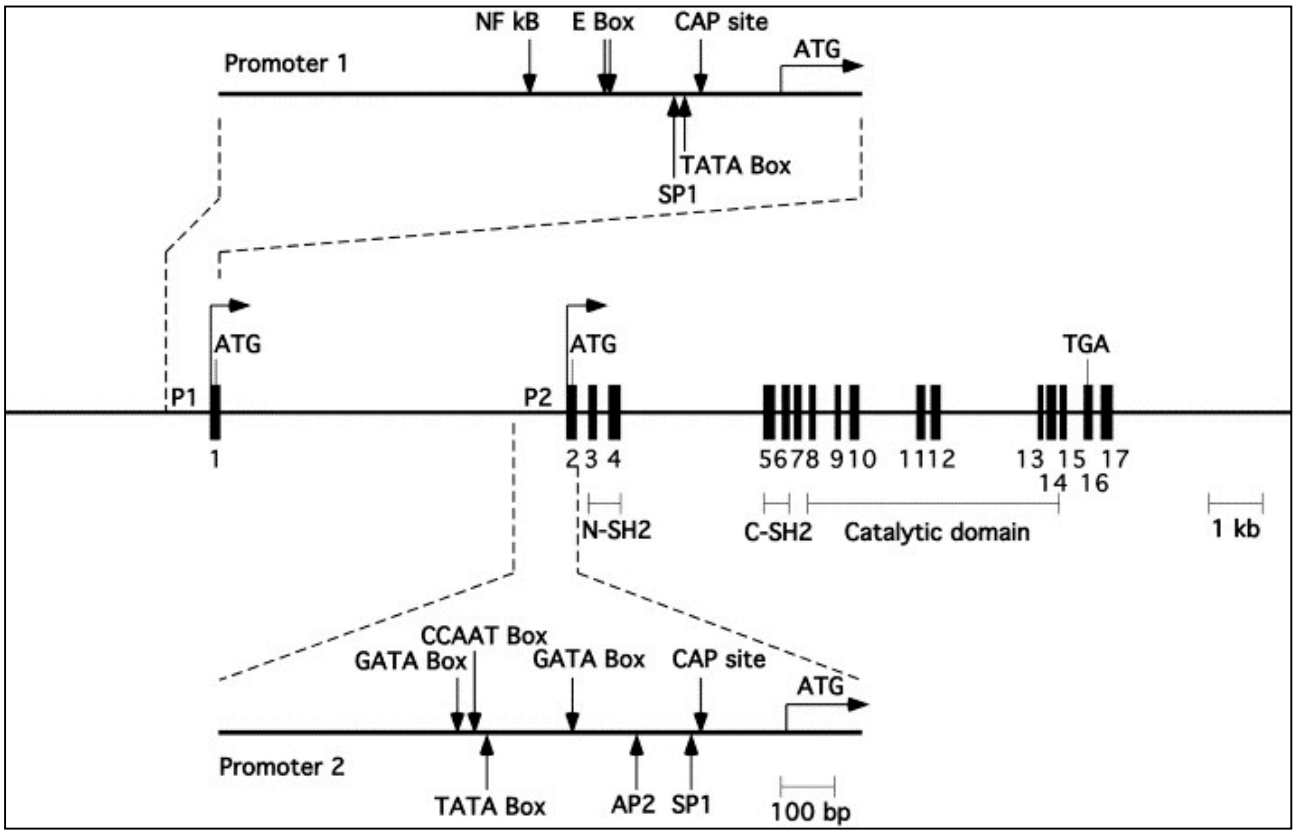

Fig.1 Schematic representation of the human SHP-1 gene. (*Wu C, Sun M, Liu L, Zhou GW, 2003).*

- **Transcription:** there are three variants of transcripts :
    1. The variant 1 represents the predominant transcript and encodes the shortest isoform.
    2. The variant 2 uses an alternate 5' terminal exon compared to transcript variant 1, resulting in an isoform (2) with a distinct and longer (by 2 aa) N-terminus, compared to isoform 1.
    3. The variant 3 uses an alternate 5' terminal exon, and an alternate acceptor splice site at the penultimate exon, compared to transcript variant 1, resulting in a longer isoform (3, also known as 70 kDa SHP-1L protein) with distinct N and C termini, compared to isoform 1.

Protein

- **Description:** SHP-1 contain two adjacent NH_2 - terminal SH2 domains, two tandem *Src* homology (SH2) domains, a catalytic domain, and a -COOH terminal tail of 100 aminoacids residues.
- **Expression:** SHP-1 tyrosine phosphatase is encoded by the PTPN6 gene and expressed primarily in the hematopoietic and epithelial cells.
- **Function:** SHP-1 plays a particularly role in the maturation and functional differentiation of lymphoid and myeloid cells as underlined by the aberrant immunoproliferation and impaired hematopoiesis in the "*motheaten*" mice that display defects in the SHP-1 gene expression. The role of PTPN6 in hematopoiesis has been shown in *motheaten* and *viable motheaten (me^v*) mice, with mutations at the SHP-1 locus. The SHP-1 mRNA from *me* bone marrow cells have a 101 bp frameshift deletion in the coding region of the N-terminal SH2 domain, while *me^v* bone marrow cells have a in-frame 15 bp deletion or a 69 bp in-frame insertion within the PTPase catalytic domain. SHP-1 acts in the immune and other hematopoietic cells by inhibiting signaling through receptors for cytokines, growth factors and chemokines as well as receptors involved in the immune responses and programmed cell death. Moreover, SHP-1 acts as tumor suppressor and loss of its expression has been identified in the whole spectrum of myeloid and lymphoid malignancies.

According to Gilfillan research, SHP-1 is found to be consitutively associated with FcεRI, with an opponing roles in FcεRI-mediated mast cell signaling. The study demonstrated that SHP-1 caused the decreased phosphorylation of FcεRI and Syk, but, also, an enhanced phohphorylation of JNK and increased the production of TNF is observed. This study, suggests that SHP-1 may play a negative role proximal to FcεRI.

It was also demonstrated that the SHP-1 protein tyrosine phosphatase negatively modulates the glucose homeostasis and insulin activity, through a dephosphorylation of transmembrane glycoprotein *Carcinoembryonic Antigen-related Cell Adhesion Molecule-1* (CEACAM-1).

The data obtained from in vitro studies of SHP-1 functions, suggested that the deficiency of SHP-1 was associated with the increase in insulin-evoked tyrosin phosphorylation of the insulin receptor, IRS-1 and IRS-2, as well as enhanced activation of PI3K and Akt in liver and skeletal muscle.

Moreover, the activation of SHP-1, through a PKC-δ and p38α MAPK actions on PDGFRβ is involved in hyperglycemia and causes an increase vascular cell apoptosis and diabetic vascular complications.

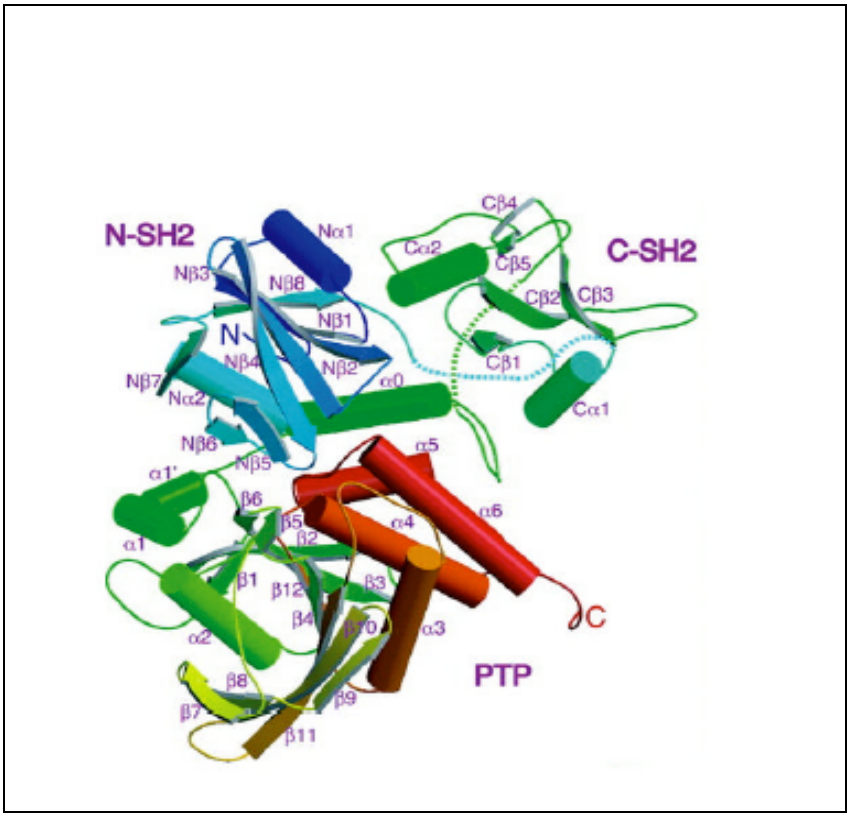

Fig.2 Crystal structure of human protein tyrosine phosphatase SHP-1. The blue region represents the N-terminal of protein, while the red region represents the C-terminal of protein.

Mutations

- **Note:** the absence or impaired function of PTPN6 in the homozygous state causes the development of the motheaten phenotype in mice, an autosomal recessive condition with focal skin inflammation and the absency of hair. Failure of neutrophils to undergo apoptosis results in the accumulation of these cells in the peripheral blood, skin, lung and spleen of affected mice.
- **Somatic:** A pathologically similar extensive skin infiltration by neutrophils is present in **Pyoderma Gangrenosum (PG)** and **Sweet's sindrome (SW)**, two uncommon neutrophilic dermatoses of unknown origin. Isoforms resulting from deletions of exons 2, 5, 11, and 15 and

retention of intron 1 or 5 were identified in a patients with a familial case of SW, who had a neonatal onset of an inflammatory disorder with skin lesions and a biopsy specimen consistent with SW. These isoforms were associated with a heterozygous E441G mutation and a heterozygous 1.7-kbp deletion in the promoter region of the *PTPN6* gene. The E441G mutation changes the hydrophilic, negatively charged amino acid glutamate to the hydrophobic nonpolar, aliphatic amino acid glycine, thereby potentially affecting the tertiary structure of PTPN6. SW an acute febrile neutrophilic dermatoses appears in several clinical forms as idiopathic, tumor associated, postinfectious and drug induced (for example after a administration of granulocyte macrophage colony stimulating factor). SW and PG have strong associations with hematological tumors. Recent studies have shown that patient with leukemia and lymphoma had methylated a P2 promoter in the PTPN6 gene, causing the absence of PTPN6 protein.

SHP-1 is expressed at low level in non-hematopoietic cells while higher levels of this protein are found in hematopoietic precursors. SHP-1 promoter methylation causes loss of SHP-1 expression in leukemias, which results in the activation of the JAK/STAT pathway. SHP-1 plays a role in **Chronic Myelogenous Leukemia** transformation and progression: it seems to be physically associated with BCR-ABL being able both to block BCR-ABL-dependent transformation and to mediate PP2A induced BCR-ABL proteosome-degradation. The tyrosine phosphatase SHP-1 plays a prominent role as resistance determinant of Imatinib (IMA) treatment response in Chronic Myelogenous Leukemia cell lines (sensitive/KCL22-S and resistant/KCL22-R).

The lack of SHP-1 expression is frequent in malignant T cells and results from methylation of the SHP-1 gene promoter. Loss of SHP1 enhances JAK3/STAT3 signaling and decreases proteosome degradation of JAK3 and NPM-ALK in ALK + anaplastic large-cell lymphoma.

According to Wu's research, in most human **Burkitt's lymphoma** cell lines, the expression of SHP-1 is decreased suggesting a role of SHP-1 in a developing of Burkitt's lymphoma, a non-Hodgkin's lymphoma, associated with EBV infection.

Moreover the activity of SHP-1, is also implicated in a breast cancer, ovarian cancer, prostate cancer, and pancreatic cancer.

Implicated in

Name: Pyoderma Gangrenosum (PG).

Disease: Pyoderma gangrenosum (PG) is a rare noninfectious neutrophilic dermatosis first described in 1930. Clinically it begins with sterile pustules that rapidly progress and turn into painful ulcers of variable depth and size with undermined violaceous borders. The legs are most commonly affected but other parts of the skin and mucous membranes may also be involved. Extracutaneous manifestations include involvement of upper airway mucosa, eye, sterile pulmonary neutrophilic infiltrates, and neutrophilic myositis . The ulcer starts as a follicular pustule with rapid growth, tissue necrosis and enlargement of the area. The surrounding skin is erythematous with infiltration end edema.

Ulcerative colitis is found in 10-15% of cases. Another associated disease is Crohn's regional enteritis with a frequency close to that of ulcerative colitis. Hepatitis C, seronegative polyarticular arthritis, spondylitis, and a broad spectrum of lymphoproliferative disorders including monoclonal gammopathies, leukemia, lymphoma, and myelodysplastic syndrome have been described in association with PG. Two main variants of PG exist: classic and atypical.

- Classic PG : characterized by a deep ulceration with a violaceous border that overhangs the ulcer bed. May occur anywhere on the body; but most commonly found on the legs.

- Atypical PG: has a vesciculopustular component only at the border, is erosive or superficially ulcerated, and most often occurs on the dorsal surface of the hands, the extensor parts of the forearms, or the face.

- **Prognosis:** Local care: debridement, intralesional injection of steroids or cyclosporin, topical agents to alter immune response (nitrogen mustard, steroids, acetic acid, 5-aminosalicylic acid) or inhibit infection. Systemic care: Glucocorticoids (prednisone). These agents have anti-inflammatory properties and cause metabolic effects. In addition, these agents modify the body's immune response to diverse stimuli. Immunosuppressives agents (Cyclosporine, Azathioprine, Mycophenolate, Cyclophosphamide, Tacrolimus, Chlorambucil) have immunomodulatory effects. These agents are used to improve the clinical and immunologic aspects of the disease. They may decrease autoantibody production and increase solubilization and removal of immune complexes. Immunomodulators (Thalidomide, Clofazimine).

Name: Sweet's sindrome (SW).

Disease: Sweet's syndrome (acute febrile neutrophilic dermatosis) is characterized by physical features, and pathologic findings which include fever, neutrophilia, tender erythematous skin lesions (papules, nodules, and plaques), and a diffuse infiltrate consisting predominantly of mature neutrophils that are typically located in the upper dermis. Sweet's syndrome presents in three clinical settings:

- Classical Sweet's syndrome (CSS) usually presents in women between the age of 30 to 50 years, it is often preceded by an upper respiratory tract infection and may be associated with inflammatory bowel disease and pregnancy.
- The malignancy-associated Sweet's syndrome (MASS) can occur as a paraneoplastic syndrome in patients with an established cancer or individuals whose Sweet's syndrome-related hematologic dyscrasia or solid tumor was previously undiscovered; MASS is most commonly related to acute myelogenous leukemia. The dermatosis can precede, follow, or appear concurrent with the diagnosis of the patient's cancer.

- Drug-induced Sweet's syndrome (DISS) most commonly occurs in patients who have been treated with granulocyte-colony stimulating factor, however, other medications may also be associated with DISS.
- **Prognosis:** The pathogenesis of Sweet's syndrome may be multifactorial and still remains to be definitively established. Systemic corticosteroids are the therapeutic gold standard for Sweet's syndrome. Horio *et al* originally described the dramatic improvement in patients with Sweet's syndrome who were treated with potassium iodide in 1980. He confirmed his earlier observations with a larger study in 1983 . Subsequently, several other investigators have also observed similar improvement when using potassium iodide to treat patients with Sweet's syndrome. Vasculitis and hypothyroidism are potential drug-induced side effects of potassium iodide. Other agents are: Colchicine, indomethacin, clofazimine, cyclosporin, dapsone.

Name: T cell lymphomas.

Disease: Cutaneous T-cell lymphoma (CTCL) is generally classified as a type of non-Hodgkin's lymphoma, and it represents a spectrum of diseases composed of malignant clonal helper T lymphocytes of the CD4 phenotype. Widely known variants include Sezary syndrome, Woringer-Kolopp disease (Pagetoid Reticulosis), CD8+ T-cell lymphoma, granulomatous slack skin, peripheral T-cell lymphoma, angiocentric lymphoma, adult T-cell leukemia/lymphoma, large-cell or anaplastic lymphoma, and lymphomatoid granulomatosis. Poikiloderma atrophicans vasculare, small and large plaque parapsoriasis, alopecia mucinosa, and lymphomatoid papulosis likely represent early forms of CTCL, but there is a problem to whether these represent CTCL or separate premalignant entities. Accurate diagnosis of early CTCL is difficult because of the varied clinical and histologic expressions of the disease and because of a lack of uniformity regarding diagnosis and treatment.

- **Prognosis:** Treatment regimens in CTCL include skin-directed therapies with UVA irradiation, topical chemotherapy with mechlorethamine (nitrogen mustard) and carmustine, and electron beam radiation, as well as systemic therapies such as chemotherapy and interferons.

Entity: Acute myeloid leukemia

Disease: Adult acute myeloid leukemia (AML) is a type of cancer in which the bone marrow makes abnormal myeloblasts (a type of white blood cell), red blood cells, or platelets. Adult acute myeloid leukemia (AML) is a cancer of the blood and bone marrow. This type of cancer usually gets worse quickly if it is not treated. It is the most common type of acute leukemia in adults. AML is also called acute myelogenous leukemia, acute myeloblastic leukemia, acute granulocytic leukemia, and acute nonlymphocytic leukemia. Most AML subtypes are based on how mature (developed) the cancer cells are at the time of diagnosis and how different they are from normal cells. Acute promyelocytic leukemia (APL) is a subtype of AML that occurs when parts of two genes stick together. APL usually occurs in middle-aged adults. Symptoms of APL may include both bleeding and forming blood clots.

- **Prognosis:** Chemotherapy is a cancer treatment that uses drugs to stop the growth of cancer cells, either by killing the cells or by stopping them from dividing. When chemotherapy is taken by mouth or injected into a vein or muscle, the drugs enter the bloodstream and can reach cancer cells throughout the body (systemic chemotherapy). When chemotherapy is placed directly into the spinal column (intrathecal chemotherapy), an organ, or a body cavity such as the abdomen, the drugs mainly affect cancer cells in those areas (regional chemotherapy). Intrathecal chemotherapy may be used to treat adult AML that has spread, or

may spread to the brain and spinal cord. Combination chemotherapy is treatment using more than one anticancer drug.

Radiation therapy is a cancer treatment that uses high-energy x-rays or other types of radiation to kill cancer cells or keep them from growing. There are two types of radiation therapy. External radiation therapy uses a machine outside the body to send radiation toward the cancer. Internal radiation therapy uses a radioactive substance sealed in needles, seeds, wires, or catheters that are placed directly into or near the cancer. Stem cell transplant is a method of giving chemotherapy and replacing blood-forming cells that are abnormal or destroyed by the cancer treatment. Stem cells (immature blood cells) are removed from the blood or bone marrow of the patient or a donor and are frozen and stored. After the chemotherapy is completed, the stored stem cells are thawed and given back to the patient through an infusion. These reinfused stem cells grow into (and restore) the body's blood cells.

To be noted

The first hint that A-to-I RNA editing has fundamental implications in leukemic disorders derives from Beghini and co-authors, who detected altered editing events in the protein tyrosine phosphatase (PTPN6/SHP-1) transcript of patients affected by AML (Galeano F. *et al. Sem Cell Dev Biol* 23, 244-250, 2012)

The analysis of PTPN6 mRNA revealed a multiple A-I editing conversion of A^{7866}, a branch site in IVS3 of PTPN6 mRNA causing the retention of IVS1.

References

1. *Protein tyrosine phosphatase containing SH2 domains: characterization, preferential expression in hematopoietic cells, and localization to human chromosome 12p12-p13*. Yi T.L., et al. Mol Cell Biol. 1992;12:836–846. PMID: 1732748
2. *Motheaten and viable motheaten mice have mutations in the haematopoietic cell phosphatase gene.* Tsui H.W., et al. Nat Genet. 1993;4:124–129. PMID: 8348149
3. *Human protein tyrosine phosphatase 1C (PTPN6) gene structure: alternate promoter usage and exon skipping generate multiple transcripts*. Banville D., et al. Genomics. 1995;27:165–173. PMID: 7665165
4. *Crystal structure of the catalytic domain of protein-tyrosine phosphatase SHP-1.* Yang J. Et al. J Biol Chem. 1998;273:28199–28207. PMID: 9774441
5. *Roles of the SHP-1 tyrosine phosphatase in the negative regulation of cell signaling.* Zhang J., et al. Semin Immunol. 2000;12:361–378. PMID: 10995583
6. *RNA hyperediting and alternative splicing of hematopoietic cell phosphatase (PTPN6) gene in acute myeloid leukemia.* Beghini A., et al. Hum Mol Genet. 2000;9:2297–2304. PMID: 11001933
7. *Treatment of pyoderma gangrenosum with infliximab in Chron's disease*. Sapienza M.S., et al. Dig Dis Sci. 2004;49:1454–1457. PMID: 15481318
8. ***SHP1** phosphatase-dependent T cell inhibition by CEACAM1 adhesion molecule isoforms*. Nagaishi T et al., Immunity. 2006 Nov;25(5):769-81. PMID: 7081782
9. *PU. 1 activates transcription of SHP-1 gene in hematopoietic cells*. Wlodarski P., et al. J Biol Chem. 2007;282:6316–6323. PMID: 17218319
10. *Sweet's syndrome–a comprehensive review of an acute febrile neutrophilic dermatosis*. Cohen P.R. Orphanet J Rare Dis. 2007;2:34–62.

11. *Decreased expression level of SH2 domain-containing protein tyrosine phosphatase-1 (**Shp1**) is associated with progression of chronic myeloid leukaemia*. Amin HM, et al. J Pathol. 2007 Aug;212(4):402-10. PMID: 17503411.
12. *A-to-I RNA editing and cancer: from pathology to basic science.* Gallo A, and Galardi S RNA Biol. 2008 Jul-Sep;5(3):135-9. PMID: 18758244.
13. . *Lyn- and PLC-beta3-dependent regulation of SHP-1 phosphorylation controls Stat5 activity and myelomonocytic leukemia-like disease*. Xiao W, et al. Blood. 2010 Dec 23;116(26):6003-13. PMID: 20858858
14. *The protein tyrosine phosphatase SHP-1 modulates the suppressive activity of regulatory T cells*. Iype T, et al. J Immunol. 2010 Nov 15;185(10):6115-27. PMID: 20952680
15. *CEACAM1: a key regulator of vascular permeability.* Nouvion AL et al. J Cell Sci. 2010 Dec 15;123(Pt 24):4221-30. PMID: 21081647
16. *Neutrophils require SHP1 to regulate IL-1β production and prevent inflammatory skin disease*. Croker BA, et al. J Immunol. 2011 Jan 15;186(2):1131-9. PMID: 21160041.
17. *The SHP-1 protein tyrosine phosphatase negatively modulates Akt signaling in the ghrelin/GHSR1a system*. Lodeiro M et al., Mol Biol Cell. 2011 Nov;22(21):4182-91. PMID: 21900501
18. *Alteration in the gene encoding protein tyrosine phosphatase nonreceptor type 6 (PTPN6/SHP1) may contribute to neutrophilic dermatoses*. Nesterovitch AB et al. Am J Pathol. 2011 Apr;178(4):1434-41. PMID: 21406173